PERFORMANCE STUDY OF ACRYLONITRILE BUTADIENE RUBBER (NBR) LATEX/ EGGSHELL FILLER COMPOSITE FILM

KUHATHASON A/L KATHIRAYSON

UNIVERSITI TUNKU ABDUL RAHMAN

PERFORMANCE STUDY OF ACRYLONITRILE BUTADIENE RUBBER (NBR) LATEX/ EGGSHELL FILLER COMPOSITE FILM

KUHATHASON A/L KATHIRAYSON

A project report submitted in partial fulfillment of the
requirements for the award of the degree of
Bachelor of Engineering (Hons) Petrochemical Engineering

Faculty of Engineering and Green Technology

Universiti Tunku Abdul Rahman

May 2019

DECLARATION

I hereby declare that this project report is based on my original work except for citations and quotations which have been duly acknowledged. I also declare that it has not been previously and concurrently submitted for any other degree or award at UTAR or other institutions.

Signature : ______________________________

Name : ______________________________

ID No. : ______________________________

Date : ______________________________

APPROVAL OF SUBMISSION

I certify that this project report entitled **“PERFORMANCE STUDY OF ACRYLONITRILE BUTADIENE RUBBER (NBR) LATEX/EGGSHELL FILER COMPOSITE FILM”** was prepared by **KUHATHASON A/L KATHIRAYSON** has met the required standard for submission in partial fulfillment of the requirements for the award of Bachelor of Engineering (Hons)Petrochemical Engineering at Universiti Tunku Abdul Rahman.

Approved by,

Signature: _________________________

Supervisor: Dr. Yamuna a/p Munusamy

Date : _________________________

ACKNOWLEDGEMENTS

Effort has been taken to complete this research, however it would not have been possible without the help of many individuals. I would like to express my gratitude to my supervisor, Dr. Yamuna a/p Munusamy, for her constant guidance and support throughout this research. Also, I would like to say thank you to all the lab staffs in Universiti Tunku Abdul Rahman for helping with this research. Finally, I like to express my gratitude to my parents, Mr. Kathirayson a/l Thiagarajah, Mrs. Jayanthi a/p Nagalingam and other members of the family for the constant support and encouragement.

Thank you.

PERFORMANCE STUDY OF ACRYLONITRILE BUTADIENE RUBBER (NBR)/ EGGSHELL FILLER COMPOSITE FILM.

ABSTRACT

The primary objective of this research is to produce acrylonitrile butadiene rubber (NBR)/ Eggshell Powder (ESP) composite film through the latex compounding and curing method. ESP loadings was varied from 0, 2, 4 to 6 phr to validate the effect of filler loading on the properties of the film. The composite films were cured at 80 oC for 120 minutes. All the composite film exhibit superior tensile strength, Young Modulus and elongation at break compared to pure NBR film, with optimum value at 4 phr loading. The dispersion of ESP in the tensile fracture was homogenous with no agglomeration observed. Resistance to chemical degradation and swelling increased with increment of filler loading. Crosslink density result showed that the higher loading of ESP filler, the crosslinking formation increased. The finding proves that ESP has a large potential to be used as a filler in latex film.

Keywords: NBR, ESP, Bio-filler, Latex Compounding Method, Chemical Degradation

TABLE OF CONTENT

CHAPTER

1. INTRODUCTION

2. LITERATURE REVIEW

LIST OF TABLES

LIST OF FIGURES

LIST OF UNITS

^{o}C	Degree Celsius
%	Percentage
$g.cm^{-3}$	Gram per cubic centimeter
lb/in^{2}	Pound-force per square inch
Psi	Pound-force per square inch
^{o}F	Degree Fahrenheit
MPa	Mega Pascal
cm^{-1}	Per centimeter
G	Gram
µm	Micrometer

LIST OF ABBREVIATIONS

3-D	Three dimensional
CAN	Acrylonitrile
Al_2O_3	Aluminium (III) oxide
$Al(OH)_3$	Aliminium Trihydrate
ATR	Attenuated total reflectance
$CaCO_3$	Calcium carbonate
$CaCO_3.MgCO_3$	Dolomite
CR	Chloroprene Rubber
EPDM	Ethylene Propylene Terpolymer
ESP	Eggshell Powder
FESEM	Field emission scanning electron microscopy
FTIR	Fourier Transform Infrared Spectroscopy
GCC	Ground calcium carbonate
KOH	Potassium Hydroxide
MgO	Magnesium Oxide
$Mg(OH)_2$	Magnesium Hydroxide
NBR	Nitrile Butadiene Rubber
NR	Natural Rubber
PCC	Precipitated Calcium carbonate
PHR	Parts per hundred rubber
PLA	Polylactic Acid
PP	Polypropylene
PSA	Particle Size Analyzer
PVC	PolyVinyl Chloride
Q_t	Molecular percent uptake

SI	Swelling index
SBR	Styrene Butadiene Rubber
TSC	Total Solid Content
UTS	Ultimate Tensile Strength
ZnO	Zinc Oxide
ZDEC	Zinc Diethyl Dithiocarbamate
ZMBT	Zinc 2-Mercaptobenzothiazole

LIST OF APPENDICES

CHAPTER 1

INTRODUCTION

1.1 Background

Over the years, problems caused by food waste has become a major concern of the food producers, food processors, retailers and even consumers. Large production of food wastes affects the food security and the food supply chain profit (Ghosh, et al., 2016). Annual world production of solid waste is around four billion tonnes and in most countries the fraction of food waste accounts for 30-45 w/w of total waste (Budhiarta, Siwar and Basri, 2012). The year in 2014, Malaysia produced food waste of 8,000 tonnes on a daily basis (The Sun Daily, 2014). On yearly basis, Malaysia is expected to produce 642,600 tonnes of food waste, and from it, up to 70,686 tonnes of eggshells were generated (Ahmad, et al., 2015).

Most of the eggshells are disposed of without any proper treatment and impart additional disposal costs to food processors. Disposal sites are hesitant to receive these eggshell wastes due to the presence of eggshell membrane which can attract pests. These eggshells can be used in many ways as it consists above 95% calcium carbonate, ($CaCO_3$) and remaining 5% organic materials. One effective approach to manage eggshell waste is applying it as bio-filler in polymeric materials. (Saeb, et al, 2010). Bio-fillers are sought after these days as they offer a sustainable and greener polymer composites. Using bio-fillers into polymer products can significantly reduce the cost of mineral fillers used from non-renewable natural resources such as lime stones and chalks (Tangboriboon, et al., 2015).

As eggshell contains 95% $CaCO_3$, it can be used as a bio-filler substitute for the commercially available mineral calcium carbonate, $CaCO_3$. $CaCO_3$, is widely available as deposits in limestone and chalks and is the most commonly used filler in polymer due to its lower price range and variety of particle sizes (Rothon, 2002). Ground Calcium Carbonate (GCC) with particle sizes ranging from 1 to 10 µm, are often used as reinforcements in polymers such as polyvinyl chloride (PVC), polypropylene (PP), elastomers such as acrylonitrile butadiene rubber (NBR), and unsaturated polyesters (Rothon, 2002). The $CaCO_3$ obtained from eggshells as said before has a lesser density: where the values obtained using ASTM-679, where eggshells had a density of 0.4236 gcm^{-3} while commercial $CaCO_3$ had density of 0.467 gcm^{-3} (Hassen, et al., 2015). This implies that the lighter product could be produced by using eggshell bio-filler compared to $CaCO_3$.

Acrylonitrile Butadiene Rubber, also known as nitrile rubber or NBR, has been known to show good performance in wide range of temperature and tends to have high resistance against oils and chemicals (Cheremisinoff, 1993). NBR was first made in the 1930's and has since shown significant growth in production and is expected to reach up to 1,562 thousand tons by the end of 2023 (Research and Markets, 2019). NBR is made by random polymerization between acrylonitrile and butadiene using the free radical catalyst. Nitrile rubber however exhibits certain limitations which include poor resistance to ketones, chlorinated and nitro hydrocarbons. The use of mineral $CaCO_3$ in NBR has shown increase in tensile strength and reduction in solvent uptake (Balachandran and Bhagawan, 2012). Eggshell can be used to replace the mineral $CaCO_3$ and can be used to improve the performance of NBR latex. Typical uses of nitrile rubber include automotive applications such as fuel and oil hoses, rollers, aircraft hose gasket, polymer films, latex gloves and in sealing products.

1.2 Problem Statement

Eggs are largely used in variety of purposes such as bakery, health products and cosmetics. Several tons of eggs are being used up every day, leaving behind eggshells as food waste, which could lead to health, land and environmental issues. Asia's consumption of eggs is said to be increasing drastically starting from 29 million tons in 2000 up to 40 million tons in 2013. As of 2013, 664, 000 tonnes of eggs were consumed in Malaysia (The Poultry Site, 2013).

The abundance of the eggshell waste has become a concern as it could cause major disposal problem. Disposal sites are hesitant to accept eggshell as the decomposition of the eggshell membranes cause smell and eventually attracts vermin (Sonenklar, 1999). Therefore, companies have to pay a high cost to the disposal site to manage the eggshell waste. Different alternatives have been used to reduce the wastage and obtain profit from these eggshells, which include using it as a calcium source for humans and animals (Brun, et al., 2013). Eggshell has also been use as soil mix compost for fertilizer (Gaonkar, et al., 2016). However these applications could not bring large reduction of eggshell waste volume due to the large amount of waste generated. Therefore, it is more practical to use eggshell as a bio-filler in polymer composite, as there is an abundance of eggshell to replace the use of mineral $CaCO_3$ filler in the polymer industry.

Calcium carbonate is one of earth's most abundantly found material. In terms of geological deposits, calcium carbonate can be found in limestone, marble, calcite chalks and even dolomite. Calcium carbonate stands as one of the most widely used fillers in the polymeric field. This broad usage of fillers can be attributed to both economic and performance wise. (Katz, et al., 1987).

According to a study made by Toro, et al. (2007), 95% of the eggshells weight consist of calcium carbonate, which can be proved to be useful as a bio-filler. The bio-fillers can be used to replace inorganic fillers as they are lower in density, has higher filling levels, non-abrasive, low in cost, and are from renewable source (Boronat, et al.,2015). A study by Boronat (2015), shows that the use of eggshell in PE improved tensile properties and impart higher degradation temperature. PVC and eggshell composites shows lower processing torque and higher thermal stability (Murugan, et al., 2016). A study using NR and eggshell shows improved tensile strength, and elongation at break (Lumlong, et al., 2016). The use of eggshell in polymer composite has proven beneficial in terms of performance and cost. Mineral $CaCO_3$ has been widely used in the glove manufacturing industry, therefore, eggshell could be a suitable replacement and will provide much benefit. One of the major market for GCC in polymer field is in gloves manufacturing industry. The annual growth rate for nitrile butadiene rubber gloves from 2017 to 2023 is expected to be 7.12% and will reach 500 million US Dollars by year 2023 (Yew, et al., 2018). NBR glove exhibit excellent heat resistance, oil and fuel resistance and superior mechanical properties compared to natural rubber gloves (Sealing Technology,2018). The study to incorporate eggshell powder bio-filler as a substitute to GCC into NBR latex film will be worthwhile pursuing.

1.3 Objectives

- To prepare eggshell powder to be used as a bio-filler in the NBR latex
- To prepare NBR latex/eggshell composite film through latex compounding methods.
- To study and determine the performance of NBR latex/eggshell composite film.

CHAPTER 2

LITERATURE REVIEW

2.1 Overview of Rubber

According to Britannica Encyclopedia, rubber is defined as an elastic substance which could either be obtained naturally from the extraction of tropical plants, or synthetically produced from the derivation of petroleum and natural gas (N. Gent, 2016). The word rubber originated from a South American Indian word, which meant weeping wood (Ciesielski, 2001). Rubber is one of the most widely used material which can produce various products such as tires for automobile, aircraft, bicycle, shoe soles, gasket, toys, medical gloves and household items. Figure 2.1 shows the vast growth in rubber use in the modern world. In 2017, 13.2 million metric tons of natural rubber was produced and consumed, whereas 15.2 million tons of synthetic rubber was produced and consumed (Statista, 2018). In the coming years the usage of rubber is expected to grow. Therefore, the demand for rubber is said to be increasing.

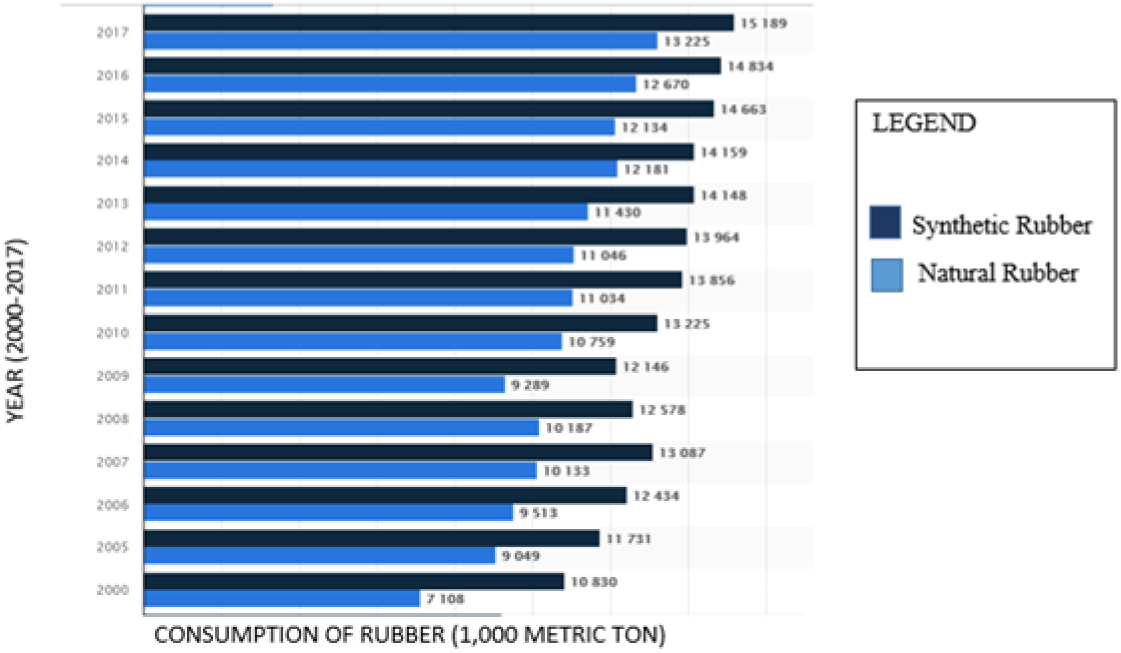

Figure 2.1: Consumption of rubber worldwide from 2000 to 2017 (in 1,000 metric tons) (Statista, 2018).

2.2 Natural Rubber

Rubber trees originated from South America, however the current leaders in rubber producers are Malaysia, Indonesia, Thailand and India (World Atlas, 2017). The production of the Natural Rubber (NR), begins when the bark of the rubber tree is slit in a way to allow the milky sap to flow. This milky sap is known as latex.

Natural Rubber latex usually contains water, polyisopropene, and other organic compounds such as protein and carbohydrates. The latex is collected in a tank and mixed with formic acid for coagulation. The coagulated latex is then pressed between rollers and dried to remove any content of excess water (NPCS Board, 2013). Natural Rubber latex is available in many grades, according to its ‘dirt’ content and production method. In simple words, the cleaner the grade (low dirt), the more expensive it is.

There has been a slight decrease in the production of natural rubber, which leads to the higher demand of synthetic rubber such as NBR. On 2018, the production of natural rubber decreased as much as 22.7% compared to the previous year (DOSM, 2018). Vulcanized rubber produced from NR has very good mechanical strength and is also elastic, enabling them to return to its original shape once the applied force is withdrawn. Other advantages of NR include high abrasion resistance, high dynamic mechanical properties and low relative cost (Kohjiya, 2014). These properties make it a good material to make tires, and vibration mounts. Natural Rubber has high impact resistance. This is because the kinetic energy of the impacting particle is converted into the deformation in shape of the vulcanite, where the energy is then released as it returns to its original state (Erman et al., 2013). However, there are certain limitations in Natural Rubber such as low ozone resistance, low ageing resistance, and non-uniform quality (Thomas, S., et al., 2014). The weakness of Natural Rubber has led to the production of synthetic rubber.

2.3 Synthetic Rubber

Synthetic rubber are usually derived from petroleum based raw material. Being produced first time in 1950, the synthetic rubber production has grown rapidly. Synthetic polyisopropene, for example, can exhibit the same properties of Natural Rubber with better purity. (Shah, et al., 2013). Some of the examples of synthetic rubber and its uses are Styrene Butadiene Rubber (SBR) used in tires and rubber hoses, Ethylene Propylene Terpolymer (EPDM) found in wire clothing and conveyer belt, Chloroprene Rubber (CR) used in water-proof rubber and window ledge, and Acrylonitrile Butadiene Rubber (NBR) used in latex glove and oil hoses (Kim, et al., 2018).

2.4 Acrylonitrile Butadiene Rubber (NBR)

Acrylonitrile Butadiene Rubber, also known as Nitrile Rubber (NBR), is made from co-polymerization of acrylonitrile and butadiene. Also known by the name Buna-N, it was first founded in Germany at 1937 by I.G. Farbenindustrie (Cheremisinoff, 1997). The structural formula of NBR is as shown in Figure 2.2.

BUTADIENE	ACRYLONITRILE
$CH_2{=}CH{-}CH{-}CH$	$CH_2{=}CH{-}CN$

NITRILE RIBBER (NBR)

$(\text{-----}(CH_2{-}CH{=}CH{-}CH_2)\text{---}(CH_2{—}CH)\text{-----})_n$

Figure 2.2: NBR Chemical Structure

NBR is formed by free-radical polymerization, as shown in the Reaction Scheme 1. Free-radical polymerization occurs through three fundamental steps: initiation, propagation and termination (Keller, 2012).

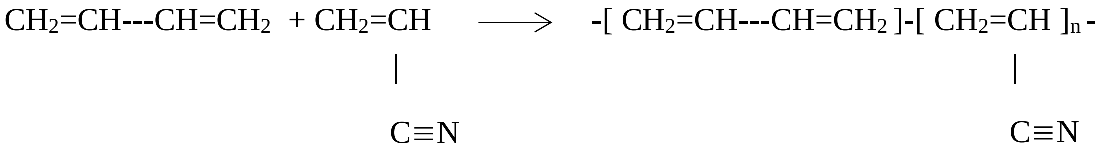

$$CH_2{=}CH{-}{-}{-}CH{=}CH_2 + \underset{\underset{C\equiv N}{|}}{CH_2{=}CH} \longrightarrow -[\,CH_2{=}CH{-}{-}{-}CH{=}CH_2\,]{-}[\,\underset{\underset{C\equiv N}{|}}{CH_2{=}CH}\,]_n{-}$$

Reaction Scheme 1: Free Radical Polymerization of NBR

NBR is produced using emulsion polymerization technique. Acrylonitrile and butadiene monomers present as emulsified droplets in a continuous water phase. Initiator is introduced to initiate the reaction and it is usually soluble in the continuous water phase, and partially soluble in emulsified phase. NBR polymer chains produced by this emulsion method has very high molecular weight. Chain transfer agents may be used to control the molecular weight of polymer to achieve desired molecular weight and viscosity of latex. The heat transfer and viscosity control are superior in emulsion polymerization compared to bulk polymerization (Keller, 2012). The NBR production is illustrated in Figure 2.3.

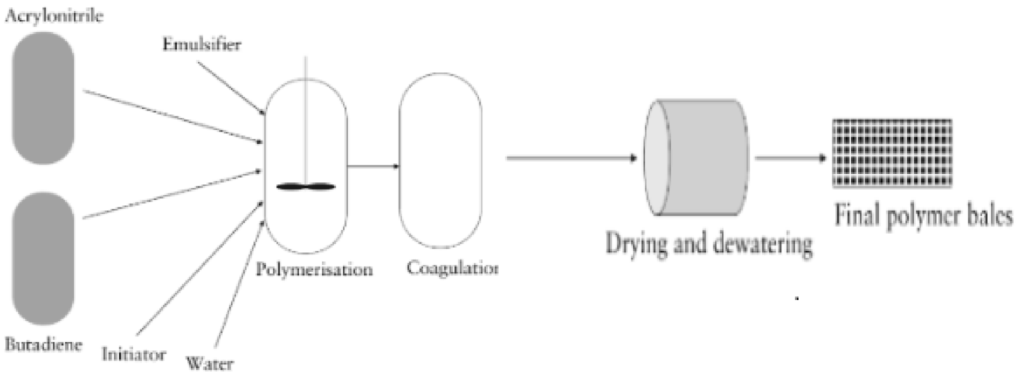

Figure 2.3: Schematic diagram of NBR production (Keller, R., 2012)

NBR has acrylonitrile content varying from 15-50%. Different content of acrylonitrile exhibit different end properties of polymer (De, White and Naskar, 2009). Acrylonitrile in the NBR makes the rubber resistant to fuels and oils such as mineral oils, grease, petroleum hydrocarbon and animal fats. Meanwhile the presence of butadiene provides resistance to abrasion and flexibility at low temperatures (Cheremisinoff, 1993). The polarity of NBR can be increased by increasing the amount of ACN. Sometimes, small quantities of rubbers such as NR, Butadiene Rubber (BR) and Styrene Butadiene Rubber (SBR) are added to improve the performance of NBR in term of weather or ozone resistance and to reduce costs (Essawy, et al., 2013). These non-polar polymers are non-compatible with NBR and do not mix, forming two separate phases. However, nitrile will easily mix with any polar materials such as PVC thus promote the production of thermoplastic elastomer with high flexibility, chemical resistant and flame retardant (Pruneda, et al., 2005). Table 2.1 shows the effect of increasing acrylonitrile content in the NBR.

Table 2.1: Effect of increasing ACN in NBR properties. (De, White and Naskar, 2009).

Physical Properties	Effect of increasing ACN level
Oil Resistance	+
Fuel Resistance	+
Hardness (Room Temperature)	+
Hardness (At 75^{o}C)	0
Tensile Strength	+
Gas Impermeability	+
Polar Materials Compatibility	+
Abrasion Resistance	+
Rebound Resistance	-
Low Temperature Flexibility	-
Compression Set	-
+: Improved Properties 0: Properties remain same -: Properties decrease	

2.5 Properties of NBR

Tensile strength of NBR increases as the ACN increases and also depends on the type of filler used. The hardness of NBR varies based on a wide range on compounding ingredient selection and increases as more ACN is added into the polymer. Elasticity of NBR is less when compared to NR or SBR. However, addition of plasticizers can improve the elastic properties of NBR (Ram Charan, 2012). With decrease in ACN content, the rebound resilience improves (Ismail, H., et al., 2014).

Nitrile rubber absorbs energy better than NR, however under long dynamic stressing, NBR vulcanizates produce heat. Abrasion resistance of NBR is better than NR and SBR. Abrasion resistance in NBR increases as the ACN content increases, and can be improved further with fillers being added (Ismail, H. et al., 2010). Table 2.2 shows the brief summary on the general properties of NBR.

Table 2.2: Properties of NBR (Nagdi, 1993)

Properties	
Density	0.0361 lb/in^2 (Base Elastomer) 0.0415-0-0488 lb/in^2 (Compounded)
Tensile Strength	130 psi @ 400^{o}F 700psi @ 250^{o}F
Elongation at Break	20% @ 400^{o}F 120% @ 250^{o}F
Glass Transition Temperature, T_g	-38^{o}C (18% ACN content) -2^{o}C (50% ACN content)
Flexibility	Good
Abrasion Resistance	Excellent
Solvent Resistance	Excellent
Oil Resistance	Excellent
Electrical Resistance	Poor
Swelling	When in contact with polar substances

One of the outstanding characteristics of NBR is their resistance to swelling when in contact with any organic liquids especially oil. The resistance of NBR varies according to the amount of ACN present, the type and amount of filler added, and the cross-link density of NBR. Oil resistance also depends on the viscosity, paraffinic and aromatic contents of the oil. High molecular weight of NBR and proper use of filler such as precipitated silica shows significant reduction in swelling properties (Promchim, et al., 2014). Polar substances such as aromatic hydrocarbons, ketones and ester can cause swelling in NBR (Wang, et al., 2014).

Flexibility of NBR at low temperatures is good due to the presence of butadiene in the polymer chain. As the content of ACN increases, the glass transition temperature of NBR also increases. The flexibility of NBR can be improved by using a low ACN count monomer and blending it with natural rubber, SBR or polybutadiene rubber (Zhang, et al., 2013).

2.6 Natural Rubber vs NBR

The properties and applications of NR and NBR are compared and contrast in Table 2.3.

Table 2.3: Properties and application of NR and NBR (Maloney Tech, 2013)

Natural Rubber		Nitrile Rubber
● Naturally produced by obtaining latex from rubber tree.	General Description	● Produced by polymerization of acrylonitrile and butadiene in a reactor.
● Excellent tensile, elongation, and electrical insulation. ● Excellent resistance to abrasion and water. ● Can be bonded to a wide range of materials. ● Good flexing at low temperatures.	Advantages	● Excellent resistance to oil, solvents and fuels. ● Good resistance to ozone with good compounding. ● Good abrasion resistance ● Resists acid and bases. ● Good resistance to heat aging ● Resistant to a broader range of aromatic hydrocarbon.
● Deteriorates when exposed to oils, fuels, solvents, or hydraulic fluids. ● Poor resistance to weather, ozone and heat.	Disadvantages	● Does not crystalize upon stretching ● Poor electrical insulation ● Poor resistance to ketones, chlorinated and nitro hydrocarbons. ● Increase in ACN reduces low-temperature flexibility.
● Used with acid and bases ● Can be used with fabric	Applications	● Mostly used as sealing products ● Industrial and automotive

and metal ● Used as electrical insulators		applications ● Chemical resistant gloves

2.7 Fillers

2.7.1 Overview

Fillers have been initially used as diluents for polymers but they were soon used to modify various properties of polymer products. Some of the most widely used fillers include, calcium carbonate, carbon black, and magnesium hydroxide. Fillers have been used extensively to reduce cost, improve processing, improve thermal conductivity, translucency, and electrical properties and flame retardancy in polymers (Kiran, et al., 2018).

Minerals are classified as inorganic fillers. Mineral fillers are usually crystalline and pure in form (Xanthos, 2010). Some of the natural mineral fillers are calcium carbonate ($CaCO_3$), dolomite ($CaCO_3.MgCO_3$), clay, talc ($Mg_3(Si_4O_{10})(OH)_2$), and calcium sulphate.

Fillers could be classified into many categories based on their shapes, sizes, chemical functional groups and origin. The fillers can also be classified into organic and inorganic families. Table 2.4 shows the organic and inorganic fillers based on their chemical family.

Table 2.4: Types of organic and inorganic fillers (Xanthos, 2010)

Chemical Family	**Examples**
Inorganic Fillers	
Oxides	Glass, MgO, SiO_2, Sb_2O_3, Al_2O_3, ZnO
Hydroxides	$Al(OH)_3$, $Mg(OH)_2$
Salts	$CaCO_3$, $BaSO_4$, $CaSO_4$, phosphates, hydroalcite
Silicates	Talc, Mica, Kaolin, Wollastonite, Asbestos
Metals	Boron, Steel
Organic Fillers	
Carbon, Graphite	Carbon fibers, Graphite fibers, Carbon nanotubes, Carbon black
Natural Polymer	Cellulose fibers, Wood flour, Flax, Cotton, Starch
Synthetic Polymers	Polyamides, Polyesters, Aramid, Polyvinyl alcohol fibers

Apart from being classified by the type of chemical family, fillers can also be classified according to various shapes and sizes, or even aspect ratio. According to Wypych (2016), there are above 70 types of particulates and flakes, and more than 15 types of natural or synthetic fibers that has been used in the polymer industry (Wypych, G., 2016). Table 2.5 shows the particle morphology of the fillers according to their shapes.

Table 2.5: Particle morphology of fillers (Wypych, 2016)

Particle Shape	Aspect Ratio	Example
Cube	10	Feldspar, Calcite
Sphere	1	Glass sphere
Block	1-4	Quartz, calcite, silica, barite
Plate	4-30	Kaolin, talc, hydrous alumina
Flake	50-200+	Mica, graphite, nanoclays
Fiber	20-200+	Wollastonite, glass fibers, carbon nanotubes, carbon fibers

A more convenient way for arranging the types of fillers is by classifying them according to their specific functions when added into polymers. These specific functions includes improvement in term of mechanical properties, fire retardants, electrical and magnetic property modifiers, surface property modifiers, and processing aids. Table 2.6 shows the type of fillers and their functions in polymers.

Table 2.6: Type of fillers according to their functions

Functions	**Examples of fillers**
Modification of mechanical properties	• High aspect ratio: glass fibers, mica, nanoclays, carbon nanotubes, carbon/graphite fibers, and aramid/synthetic/natural fibers • Low aspect ratio: talc, $CaCO_3$, kaolin, wood flour, wollastonite, and glass spheres
Enhancement of fire retardancy	• Hydrated fillers: $Al(OH)_3$ and $Mg(OH)_2$
Modification of electrical and magnetic properties	• Conductive, nonconductive, and ferromagnetic: metals, carbon fiber, carbon black, and mica

Modification of surface properties	• Antilock, lubricating: silica, $CaCO_3$, PTFE, MoS_2, and graphite
Enhancement of processability	• Thixotropic, antisag, thickeners, and acid • Scavengers: colloidal silica, bentonite, and hydrotalcite
Permeability control	• Reduced permeability: impermeable plate-like fillers: mica, talc, nanoclays, glass flakes • Enhanced permeability: stress concentrators for inducing porosity: $CaCO_3$ and dispersed polymers
Bioactivity	• Bone regeneration: hydroxyapatite, tricalcium phosphate, and silicate glasses
Degradability	Organic fillers: starch and cellulosic fibers
Radiation Adsorption	• Metal particles, lead oxide, and leaded glass
Improved dimensional stability	• Isotropic shrinkage and reduced warpage: particulate fillers, glass beads, and mica
Modification of optical properties	• Nucleates, clarifiers, and iridescent pigments: fine particulates and mica/pigment hybrids
Damping control	• Flake fillers, glass, and $BaSO_4$

2.7.2 Calcium Carbonate ($CaCO_3$)

Calcium carbonate is one of the most widely used fillers in the polymer industry, due to its low cost and wide range of particle sizes (Gerrard, 2001). It can be found throughout the world and compromises of 4% of the earth's crust. Some of the natural source of calcium carbonate include limestone, marble and chalk (Brewis et al., 2012). Calcium carbonate takes up 55% of polymer filler sales (Brewis et al., 2012). It is mainly used as fillers for PVC, Polypr, unsaturated polyesters and elastomers (DeArmitt, C., et al., 2016).

Calcium carbonates can be present in few crystalline forms: calcite, aragonite and a less common type vaterite. (Kitamura, 2001). The most commonly used calcite has density 2.7 kg/L, Moh hardness 3, and refractive index 1.57 (DeArmitt, C., et al., 2016). Calcite can be produced from mineral rocks such as limestone, marble and chalk. Aragonite, specific gravity of 2.92-2.94 kg/L, Moh hardness of 3.5 up to 4.0 (Carr and Frederick, 2000). Commercially calcium carbonate are prepared as Ground Calcium Carbonate (GCC) and Precipitated Calcium Carbonate (PCC) to be used in polymers. GCC is often used in plastics even without surface treatment. GCC is produced from milling chalk to break down chalk to finer structures. Further processing will be done for the reduction of size (BCCF, 2018). Fillers produced through this method are called whiting. CC particles can be coarse, sometimes up to 100µm in size.

PCC is produced for finer grade fillers and chemically it is pure calcium carbonate. It is produced by heating or calcining the natural form of limestone, to form calcium oxide (quicklime). The calcium oxide is then mixed with water to form calcium hydroxide in slurry form. The slurry calcium hydroxide is then passed through carbon dioxide, where it will precipitate to form calcium carbonate. Slur is then dried out, producing fine powders (Grossman, et al., 2000).

GCC is the most used filler in plastic industries and its most common form is calcite. Calcite contains up to 94-99% of $CaCO_3$, with the remaining impurities such as alumina, magnesium carbonate, silica and iron oxide. As for PCC it contains mainly aragonite, and has ~~a~~ higher purity as it contains 98-99% of $CaCO_3$ (Minerals Technologies, 2019). PCC is sometimes preferred over GCC due to its high purity content, constant and regular particle shape, narrow particle size distribution and also has high surface area, due to its fine particles. (Shi et al., 1994). However, PCC is costly and is not used widely as compared to GCC. In Europe, around 97% by weight of calcium carbonate used are GCC, while the remaining 3% are PCC. (Brewis et al., 2012).

2.7.3 Organic Bio-Fillers

Before, most polymer products were obtained from petrochemical sources. However, these days community in general prefer the use of naturally occurring products. Inorganic fillers from non-renewable natural resources are being replaced in favor of bio-fillers, such as eggshell, shellfish shell, kenaf powder, coconut husk and many more, due to their superior properties such as improved mechanical performance, high filling levels, and low density (Boronat et al., 2015).

Boronat, (2014), had developed bio-composite based on green polyethylene biopolymer and eggshell bio-filler. Their result concluded that the use of modified eggshell as filler showed significant improvement in mechanical properties such as stiffness, hardness, flexibility and tensile strength.

Stevulova et al. (2015), has studied the use of chemically treated hemp shives as a suitable organic filler for lightweight composites preparation. Somdee and Hasook (2017) had studied the use of modified eggshell powder on physical properties of poly(lactic acid) and Natural Rubber composites. With increasing loading of eggshell bio-filler, the composite showed higher Young's modulus and elongation at break. However addition of modified eggshell powder in the Natural Rubber composite had decrease the impact strength.

Iheoma (2015), had studied on the mechanical properties of carbonized and uncarbonized corn hub powder filled natural rubber/ acrylonitrile butadiene rubber bio-composite. The addition of corn hub powder in the composite had shown an increase in tensile strength, abrasion resistance, hardness and elasticity. However rebound resilience, elongation at break and compression properties showed slight decrement.

2.8 Food Wastes

Over the years, the increasing amount of food waste has been a significant problem, and if not treated and handled properly, can cause serious health and environment issues. Most of the food waste come from the food processing factories, agricultural industry and households (Arvanitoyannis, 2008). Malaysian households produce up to 30,000 tonnes of solid waste, in which 47% of it consists of food waste (Mohamed, 2015). The food wastes include foods leftover after meals, such as chicken bones, eggshells, and fruits skin.

One of the major contributors of food waste is eggshells. The production of chicken eggshells in Asia has been growing rapidly, according to Global Poultry Trend. The production of eggs in Asia has increased from 29 million to 40 million tons. (The Poultry Site, 2014). In 2010, Malaysia has produced more than 30,000 metric tons of chicken. These production has led to the growth in number of eggshells. Eggshell disposal without being treated, can cause unpleasant smell, attract growth of bacteria and cause problems to environmental and health (Mohamed, 2012). One of the steps that can be taken to reduce the problems related with eggshells are by using them and recycling them into useful products.

2.9 Eggshell Composition

The whole egg consists of three parts: the eggshell which is 9-11%, egg white which is 60-63% and the yolk which makes up 28-29%. Eggshells include the shell membrane which is in between the inner shell surface and the albumen (Mine, 2008). Yolk is located in the middle of the egg, surrounded by the eggshell membrane, which is then covered by the hard surface of the eggshell. The main purpose of the eggshell is to provide protection to the contents in it against predators and microorganism (Hincke, 2012). The eggshell and eggshell membrane has different chemical composition.

Eggshell consists of 94-95% calcium carbonate in calcite form. The remaining components of the eggshell include inorganic components such as magnesium carbonate, calcium phosphate. The eggshell is one of the major source of calcium for animals or even soil compost (Baláž, 2014). The eggshells have 7000-17000 pore canals distributed evenly on its surface which functions in gas and water exchange. (Mine, 2008). Figure 2.4 shows the structure of the egg and its shell.

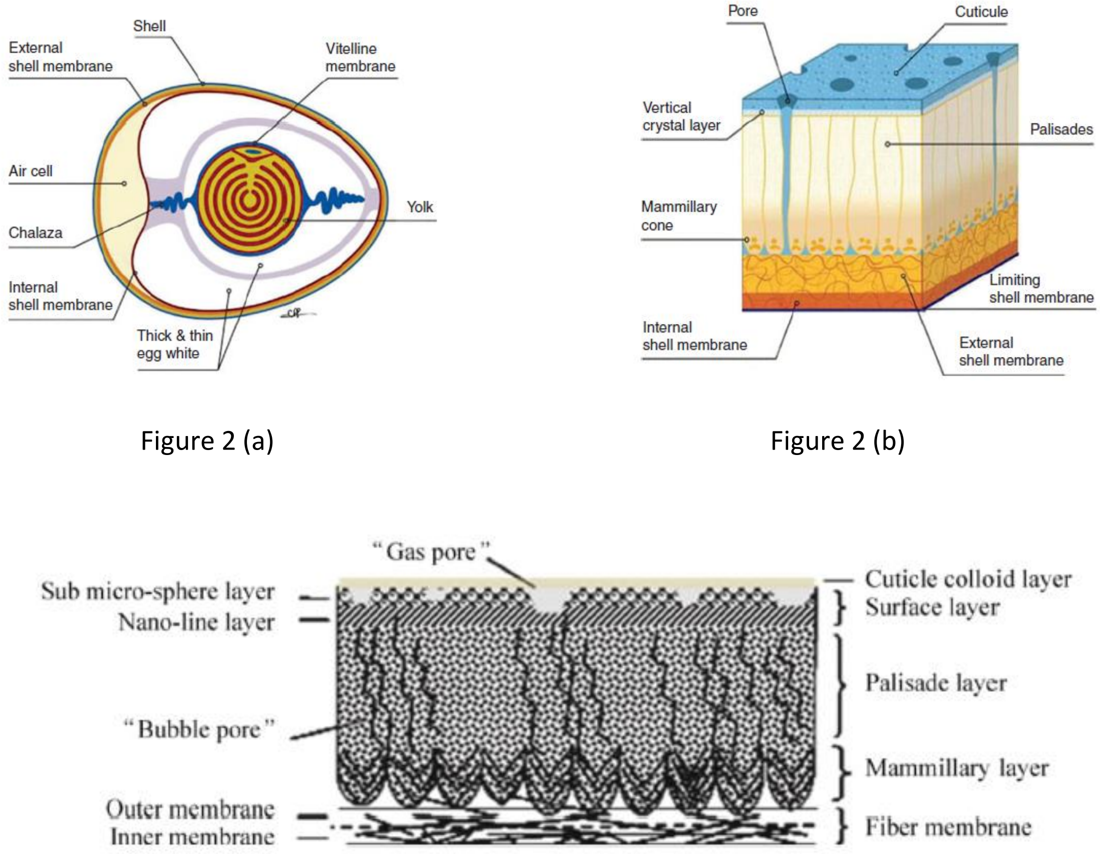

Figure 2 (a)

Figure 2 (b)

Figure 2 (c)

Figure 2.4: (a) & (b) Structure of eggshell (Hincke, 2012),

(c) Detailed schematic diagram of eggshell (Baláž, 2014).

Eggshell membrane has two parts, the inner and outer membrane with an entangled like structure which functions in trapping microorganisms. The eggshell itself can be divided into three layers: the surface, palisade and mammillary layer, which is in the form of calcite. (Clark, et al., 2014). Mammillary layer, which is the innermost, has an approximate 100µm thickness and grows on the outer layer of the membrane. It creates the base for the thickest palisade part, which is around 200µm of thickness. The top outer most layer consists of organic cuticle and is around 5-8µm of thickness (Izumi et al., 1994). Figure 2.5 shows the Field Emission Scanning electron microscopy (FESEM) image of the eggshell layers.

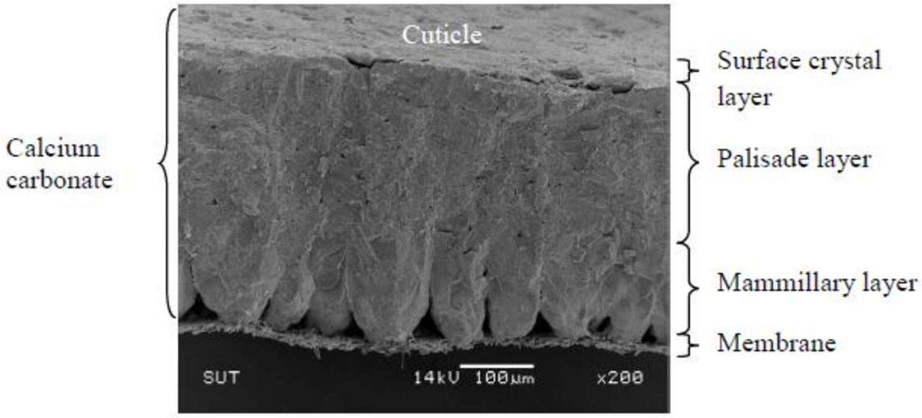

Figure 2.5: FESEM image of chicken eggshell structure (Dennis, et al., 1996).

2.10 Eggshell as Bio-Filler

The use of eggshell as calcium carbonate filler substitute will reduce the cost of purchasing commercial grade filler for polymer industry. The market price of the precipitated calcium carbonate obtained from limestone is around 120 euros per ton (Teir, 2005). Thus, the chicken eggshell from waste can be used by turning it into a valuable product to replace $CaCO_{3.}$ Other bio-fillers which consists of calcium carbonate has been used previously, such as shrimp shell and shellfish shell. Based on several research, the use of fine shellfish shell as filler in PP composite can increase the mechanical properties of the polymer (Li et al, 2012). But when compared to eggshell, the process for obtaining the filler is complex as the organic membrane are too hard to be removed from the shrimp shell and shellfish shell. Pre-treatment of these shells even use high amounts of chemicals and solvents, which could cause a rise in the cost of filler production. When compared to chicken eggshell, the process is much simpler, as it was grinded and washed with water to remove any remaining membranes. The use of chemicals and solvent in pre-treating the shrimp and shellfish shells could pose danger to the environment due to the discharge of these chemicals. (Bashir et al., 2015).

2.10.1 Effect of Filler in Elastomer

Fillers are important in the production of elastomers products. Some of the major fillers used in the elastomer fields include carbon black, silica, clays and calcium carbonate. The main use of these fillers are to reduce cost and increase mechanical properties, such as modulus, abrasion resistance, tear strength and tensile strength. Due to the frequent use of elastomers in dynamic applications, these mechanical properties are of great importance (Chukwujike et al, 2015).

The effect of eggshell powders on elastomers such as NR and SBR have been studied. According to Somdee and Hasook (2017), addition of modified eggshell powder on physical properties of poly(lactic acid) and natural rubber composites, the addition of modified eggshell as filler in the PLA/NR composite have shown a decrease in the elongation of break. By increasing the MES content in the PLA/NR composite, tensile strength at break has decreased from 47 MPa to 6 MPa. The Young's modulus in the composite was higher with the addition of MES compared to neat PLA. Impact strength has decreased when included the MES was incorporated in the PLA/NR composite.

SBR composite was developed with adding eggshell as bio-filler was studied at different loading. The thermo-mechanical properties of the eggshell was compared to the SBR prepared by calcium carbonate filler. Incorporation of eggshell as filler has showed improvement in the tensile strength and elongation at break. Higher thermal stability was observed in samples with 5 phr loading of eggshells, compared to the same thermal stability showed when using 10 or 15 phr of calcium carbonate filler (Mohammad et al, 2010).

CHAPTER 3

METHODOLOGY

3.1 Introduction

In the process of studying the performance of latex, it became known that there are a few methods to the membrane casting. This chapter includes the description of selection of the membrane casting method used, preparation of ESP, characterization of ESP and composite film and also the performance study of composite film. The complete methodology is summarized in Figure 3.1.

3.2 Process Flow Chart

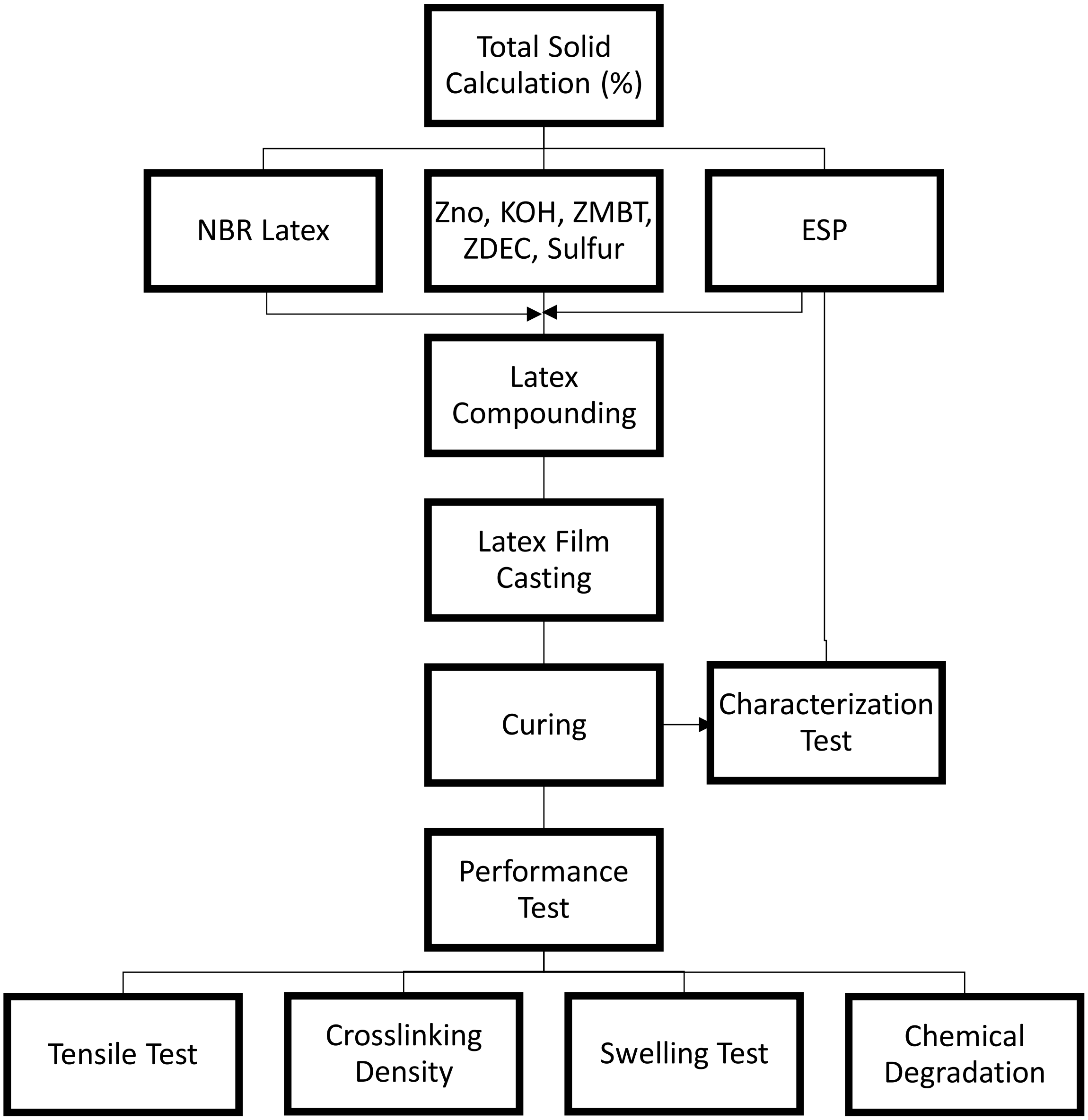

Figure 3.1: Flowchart of Process Flow

NBR = Nitrile Butadiene Rubber

ESP = Eggshell powder

ZDEC = Zinc Diethyldithiocarbamate

ZNO = Zinc Oxide

KOH = Potassium Hydroxide

ZMBT = Zinc 2-Mercaptobenzothiazole

3.3 Raw Material for Composite Film Preparation

The raw material used in the compounding of composite film includes NBR with TSC 60.82% provided by Synthomer Sdn. Bhd. The Potassium Hydroxide (KOH), Zinc 2-Mercaptobenzothiazole (ZMBT), Zinc Diethyldithiocarbamate (ZDEC), Zinc Oxide (ZnO) and Sulfur were all purchased from Zarm Scientific & Supplies Sdn. Bhd. Malaysia. Eggshells were collected from restaurants around Kampar, Perak, Malaysia. Table 3.1 shows the function of each compounding agents.

Table 3.1: Compounding Material and their Functions

Material	**Function**
NBR	Polymeric material base to be casted in film
KOH	Acts as stabilizer to control acidity of latex and prevent coagulation of latex
ZMBT	Secondary accelerator acts to give vulcanizates of higher modulus
ZDEC	Primary accelerator to reduce vulcanization time and temperature
Zno	Activates sulfur crosslinking formation and improve vulcanization efficiency
Sulfur	Crosslinking agent acts to initiate crosslinking formation in latex solution

3.4 Preparation of NBR/ESP Composite Film

3.4.1 TSC Calculations

NBR latex is in emulsion form which consists of latex particles dispersed in water based system. ZDEC, ZMBT and ZNO are in slurry form. Thus to perform latex compounding, the total solid content of each component had to be calculated.

Approximately 2 g of NBR, ZDEC, ZMBT and ZNO component were placed on separate evaporating dishes. Initial weight of each chemical components was measured. All ingredients were placed in drying oven model Memmert Incubator Oven INB200 at 100^{o}C for 2 hours. Then, the ingredients were removed from oven, cooled to room temperature for 15 minutes, and were weighed. The ingredients were then placed in oven again at 100^{o}C for another 15 minutes. This step was repeated until a constant value of weight is obtained. TSC were calculated using Equation 3.1.

$$\text{Total Solid Content (\%)} = \frac{Dry\ Weight\ of\ Component}{Wet\ Weight\ of\ Emulsion/Slurry} \text{ x } 100\%$$

Equation 3.1

TSC was calculated for all components except KOH. Since KOH is present in dried pellet form, the solution is determined by dilution method. To obtain 10% of KOH TSC, 10 g of KOH is added to 90% of distilled water and is diluted.

Upon calculating TSC for each component, the actual mass of suspension required in compounding of latex. The compounding ingredient formulation based on actual mass is as stated in Table 3.2. Calculated TSC value for components are recorded in Table 3.3.

Table 3.2: TSC Calculation

$Desired\ Weight = \frac{TSC\%}{100\%} \times Actual\ Weight$

Desired weight is weight required based on set composition

$$Actual\ Weight = \frac{Desired\ Weight\ \times 100\%}{TSC\%}$$

100 phr = Desired weight of NBR

$$1\ phr = \frac{Desired\ weight\ of\ NBR}{100}$$

$$Desired\ weight\ of\ component = \frac{Desired\ weight\ of\ NBR}{100} \times formulation$$

$$Actual\ Weight = \frac{Desired\ Weight\ of\ NBR}{100} \times formulation\ \times \frac{100\%}{TSC\%}$$

$$Actual\ Weight = \frac{Desired\ Weight\ \times 100\%}{TSC\%}$$

Table 3.3: TSC values of Component

	phr formulation	Dry Weight (g)	Actual Weight (g)	TSC (%)
NBR	100	60.8202	100	60.82
KOH	1	0.6082	6.082	10.00
ZNO	1	0.6082	1.267	47.98
ZMBT	0.5	0.3041	1.054	57.69
ZDEC	1	0.6082	1.108	54.86
S	1	0.6082	1.087	55.97
ESP	0	0	0	100
	2	1.2164	1.2164	100
	4	2.4328	2.4328	100
	6	3.6492	3.6492	100

3.4.2 ESP Preparation

The eggshell was washed in running tap water to remove any contaminants on its surface. The membrane in the inner shell was removed using hand. The eggshells were then left to dry overnight at room temperature to remove excess water. Then eggshells were blended using Waring Laboratory Blender Model HGB 2WTS3 to smaller pieces and dried in Universal Oven Model U supples by Memmert GmBH at 100 ˚C for 5 hours.

The dried eggshell was grinded to powder using Ultra Centrifugal Mill ZM200 from RETSCH GmBH Company, Germany. The grinded samples were then sieved using 0.1 µm mesh W.S Tyler's RO-TAP® Sieve Shaker Model RX-29-10 from United States and was stored in a dry place prior to usage.

3.4.3 NBR/ESP Compounding

Formulations to prepare the latex films are listed in Table 3.3. Pure NBR film was prepared as control sample to compare the effects of adding eggshell powder as filler. NBR latex was compounded using mechanical stirrer model IKA RW 20 Digital. First, KOH was added into the NBR latex and stirred at 220 RPM. After five minutes, the remaining compounding agents such as ZMBT, ZDEC and ZnO were added. As Sulfur promotes cross-linking, it is added lastly to the NBR mixture to prevent it from becoming too viscous. Stirring was continued for another 30 minutes at speed ranging from 200 to 250 rpm.

For the NBR film with ESP, firstly, the NBR latex was stirred with KOH at 220 rpm, then the ESP was added into NBR followed by the other compounding ingredients such as ZMBT, ZDEC, Sulfur and ZnO. The stirring speed and time to compound the NBR/eggshell latex is the same as for the pure NBR film.

3.4.4 Casting of Composite Film

The NBR and NBR/ESP compounds were used to cast the films using the membrane auto casting machine, from Autonics Corporation. The gap of the casting knife was set to 150 µm and was placed in front of moving beam, where the compounded latex was evenly distributed on the glass plate by the casting knife. The speed of the moving beam was fixed at 150 rpm and the process distance was set to 240 mm. The thickness of the film is set to 0.10 mm. After 15 minutes under room temperature, the glass plate with film was placed into the drying oven model Memmert Incubator Oven INB 200 for 2 hours for curing purpose at temperature of 80^{o}C.

3.5 Characterization of Filler

3.5.1 Particle Size Analysis (PSA)

Particle size of the eggshell powder was measured using Mastersizer 2000, Hydro2000 MU (A) Particle Size Analyzer and the refractive index used was 1.36. In order to determine the particle size present in the eggshell powder, the particle size analyzer was used, as it is suitable to determine particles in the size range of 0.02µm to 2000 µm. (Brummer et al., 2008).

3.5.2 Thermal Gravimetric Analysis (TGA)

TGA model Mettler Toledo TGA is used to determine the thermal decomposition pattern and temperatures for eggshell powder. The eggshell powder was heated up to 800 ^{o}C under the flow of nitrogen at the heating rate of 20 °C/min (Chai et al., 2016).

3.5.3 Field Emission Scanning Electron Microscopy (FESEM)

Field Emission Scanning Electron Microscopy is used to observe the morphology of the eggshell powder. High-energy electron beams is generated at the surface of the ESP to generate various signals, and the two-dimensional image is generated. The equipment model used was JSM 6701F supplied by JEOL Ltd.

3.5.4 Fourier Transform Infrared Spectroscopy (FTIR)

Fourier Transform Infrared Spectroscopy is used to analyze the types of functional groups and chemical interactions in the eggshell powder. FTIR analysis was carried out using Spectrum RX1 Perkin Elmer analyzer. The absorption frequency range of FTIR was set to 4000 cm^{-1} to 400 cm^{-1} at room temperature. The powder sample was analyzed using KBr method for 32 scans.

3.5.5 X-Ray Diffraction

X-Ray Diffraction analysis carried out in this study was performed using Siemens XRD Diffractometer 5000 which operates using Nickel filtered copper Kα radiation with $\lambda = 0.154$ nm. The samples were scanned between 10-60˚ at scanning rate 2˚/min.

3.6 Characterization of Composite Film

Fourier Transform Infrared Spectroscopy - Attenuated Total Reflectance (FTIR-ATR) is used to analyze the functional groups and types of chemical interactions in the NBR/ESP film. In this test, Thermo Fischer Scientific FTIR spectrometer with ATR mode was used and the analysis was conducted in room temperatures at band frequency range of 4000 cm^{-1} to 400 $cm^{-1}$for 32 scans. XRD was performed on the NBR/ESP composite film using the same equipment model and testing parameters as reported in Section 3.5.5.

3.7 Performance Test

3.7.1 Tensile Test

Tensile test was carried out to determine the ultimate tensile strength (UTS), elastic modulus and percentage elongation at break of the composites. The tensile test was conducted using Tinius Olsen H10KS-0748 light weight tensile tester machine. The test was carried out according to ASTM D412 test method using dumbbell shaped test specimens at a uniform speed of 100mm/min, load 450 N, 1200 extension length limit and 26 mm gauge length.

3.7.2 Swelling Test

Swelling test is used to measure the swelling behavior of the film composite in solvent and performed based on ASTM D3616--95. It is measured by the change in mass of samples under the exposure of chemicals. Samples were immersed in toluene and n-hexane under ambient temperature for 5 days. After that samples were quickly removed, wiped and weighed. The samples were further dried in an oven for 24 hours at temperature of 60 °C. Dried samples were cooled and weighed. The swelling resistance of film composite were calculated and recorded using Equation 3.3

a) Molecular % uptake, Qt (%) = $\frac{(w_2-w_1)/W_m}{w_1} \times 100\%$ Equation 3.2

b) Swelling index, SI (%) = $\frac{w_2-w_1}{w_1} \times 100\%$ Equation 3.3

where:

w_1= initial weight

w_2= swollen weight

W_m= molar mass of solvent

3.7.3 Crosslinking Density

Crosslinking density was calculated using equilibrium swelling method with acetone according . Initial weight of film composite samples were measured and immersed in acetone for 72 hours. After a period of 72 hours, the film was taken out, wiped with filter paper, and immediately weighed. All solvent was removed by drying in oven at 100°C, and is reweighed. The density of the film is measured using density kit. Flory-Rehner equation in Equation 3.4 and 3.5 shows the step to calculate crosslinking density of composite film (Ain and Azura, 2010).

$$\text{Volume Fraction, } V_r = \frac{\left(\frac{m_1}{\rho_r}\right) - V_f}{\left(\frac{m_1}{\rho_r}\right) - V_f + \left(\frac{m_2 - m_3}{\rho_s}\right)} \qquad \text{Equation 3.4}$$

where: m_1 = Initial weight of specimen

m_2 = Weight of swollen specimen

m_3 = Weight of specimen after equilibrium

V_f = Volume of filler

ρ_r = Density of rubber

ρ_s = Density of solvent

Crosslinking Density, $n = -\frac{ln(1-V_r)+V_{r+}\mu V_r^2}{V_0[(V_r)^{\frac{1}{3}}-\frac{V_r}{2}}$ Equation 3.5

where: μ: NBR-Acetone interaction parameter

V_0: Molar Volume of Acetone

3.7.4 Chemical Degradation

Chemical degradation test was carried out according to Ansell Test Method for latex gloves based on Standard EN374-4:2013 for latex gloves. NBR films were cut in square shape and the initial weight of the film was measured. The test chemicals used in this test are 10% Hydrochloric Acid (HCl), 10% Acetic Acid (AA), 50% Sodium Hydroxide (NaOH), Turpentine and Kerosene. The film were completely immersed in test chemicals for around 30 minutes. The film is then dried using filter paper and the weight after being immersed in chemical is measured to calculate the percentage of weight change in accordance to Equation 3.6.

$Weight\ Change(\%) = \frac{Final\ weight-Initial\ weight}{Initial\ Weight} \times 100\%$ Equation 3.6

CHAPTER 4

RESULT AND DISCUSSION

4.1 Characterization of Filler

Particle Size Analysis was conducted to determine the particle size of ESP filler. Figure 4.1 (a) and (b) shows the particle size of ESP and commercial $CaCO_3$ respectively. The mean distribution size at peak $d_{0.5}$ for commercial $CaCO_3$ is 18.382 μm, while the mean distribution at peak $d_{0.5}$ for ESP is 16.183 μm. This shows that ESP has a smaller particle size, which in return has a bigger surface area. The smaller the filler's particle size, it can contribute more to the enhancement of mechanical properties and increase the strength (Fu et al., 2008). This is due to improved filler matrix interaction between the NBR chain and ESP surface (Zaini et al, 1996).

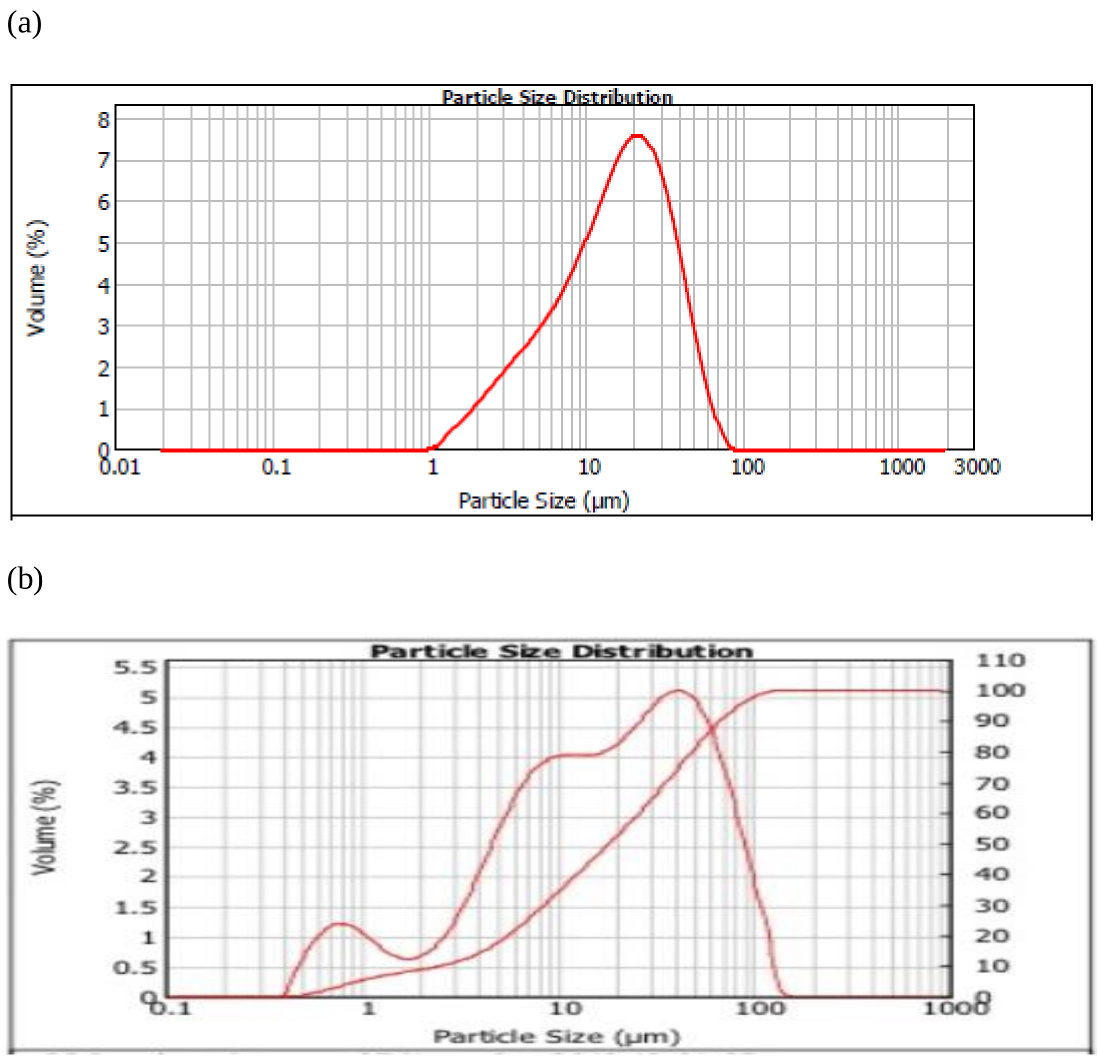

Figure 4.1: (a) PSA of ESP and (b) PSA of commercial $CaCO_3$ (CRC,2012)

ESP is tested using TGA to determine its decomposition temperature (Ahmad, Rohim and Ibrahim, 2015). It can be observed that there was a slight decrease in the curve due to the loss of surface and inbound water molecules at temperature below 200˚C. At around 300ºC the weight loss is due to the decomposition of residual organic protein molecules. These organic proteins tend to decompose from organic fractions into small molecules such as CO or CO_2 (Naemchan, 2008). Above 600ºC, the drastic weight loss in curve is due to the decomposition of the calcium carbonate to calcium oxide (Freire and Holanda, 2006).

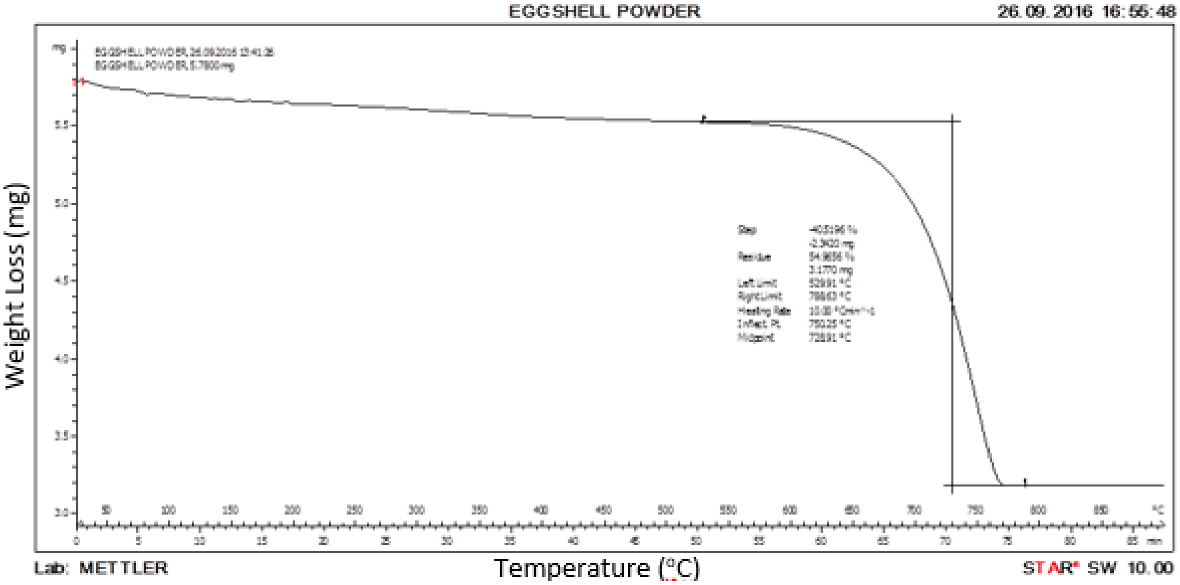

Figure 4.2: TGA curve of ESP

FESEM was used to test and identify the morphology of ESP. Based on the observation in Figure 4.3, chicken ESP had irregular shape. The morphology of the ESP is similar to commercial $CaCO_3$ (Bootklad, M. et al., 2013). The irregular shape present in ESP can provide better interaction and physical interlocking of polymer chains on the surface of the filler, which can aid in achieving excellent mechanical properties (Iyer, K.A., et al., 2014).

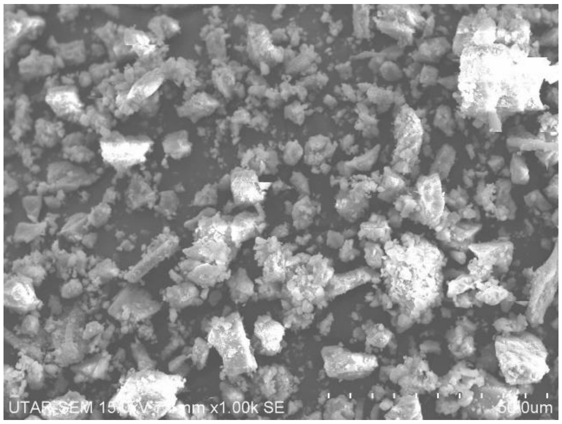

Figure 4.3: FESEM image of ESP at magnification of 1,000X.

The FTIR peaks for ESP is shown in Figure 4.4 and summarized in Table 4.1. Peak at wavelength 3432 cm^{-1} represents the O-H hydroxide bond caused by the vibration of water molecules (Chakraborty et al., 2007). The CO_3^{2-} ion is commonly present in $CaCO_3$ and the related absorption peak can be observed at 712 cm^{-1} and 1420 cm^{-1}. These absorption are highly associated with carbonate minerals in the ESP (Tsai, W.K., et al., 2006). Absorption peak at 875 cm^{-1} indicates the presence of calcite in $CaCO_3$.

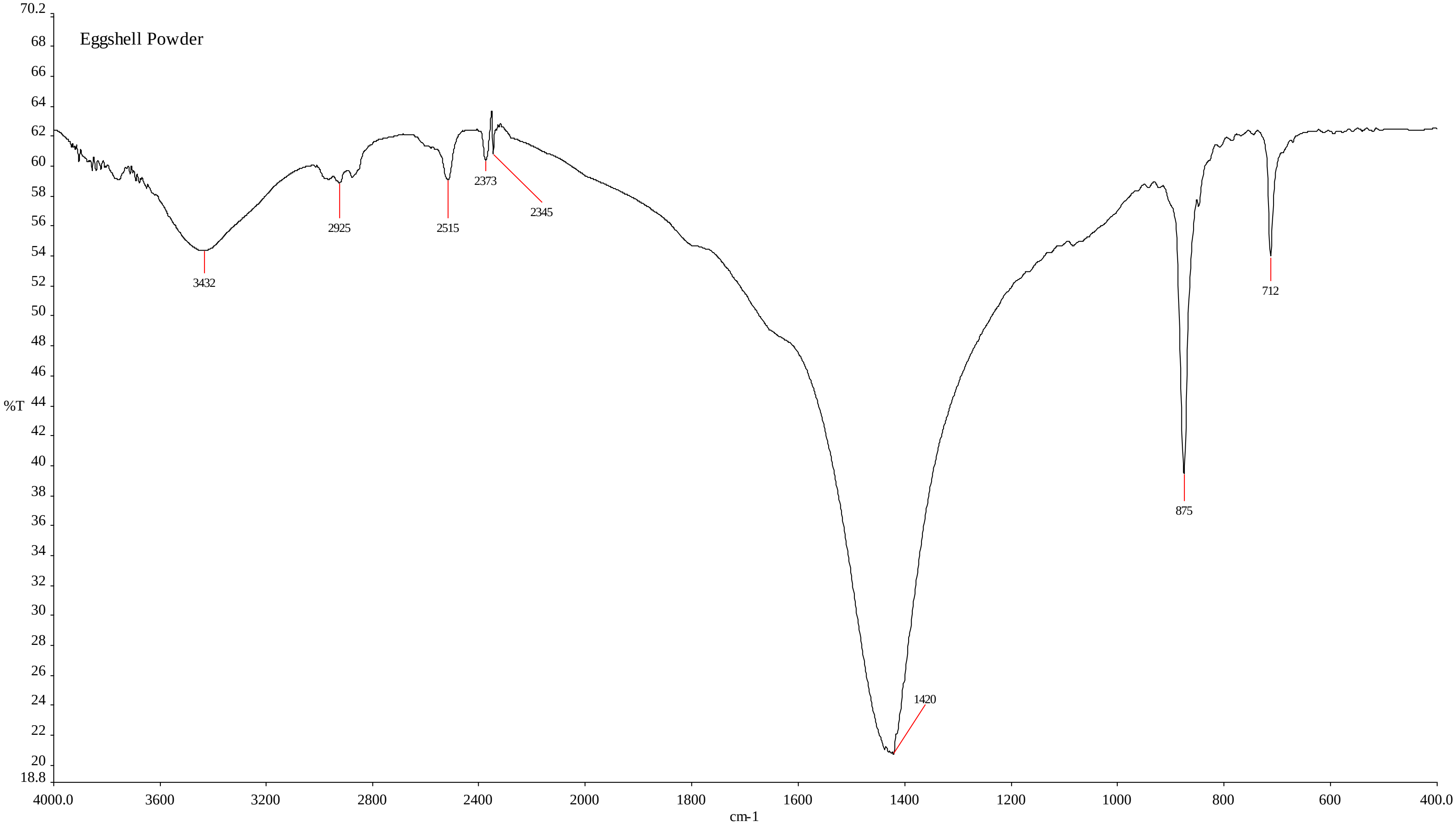

Figure 4.4: FTIR curve of ESP

Table 4.1: Absorption Frequency Regions and Functional Groups of Eggshell Powder (ESP).

Absorption Frequency Range (cm^{-1})	Absorption Frequency (cm^{-1})	Functional Group
	Eggshell Powder (ESP)	
3200-3550	3432	Alcohol O-H bond stretching
2840-3000	2925	Alkane C-H bond stretching
2500-3300	2515	Carboxylic Acid O-H bond stretching
~2349	2345, 2373	Carbon Dioxide O=C=O bond stretching
1330-1420	1420	Alcohol O-H bond bending
880 ± 20	875	Carbonate, CO_3^{2-} C-H bending
665-730	712	Alkene C=C bond bending

XRD test showed that the major composition of the eggshell consist of $CaCO_3$ in Figure 4.5. Peak of calcite observed in ESP is at the same range in commercial $CaCO_3$ (Thriveni, et al, 2014). The XRD peaks confirmed that ESP has similar crystalline structure as the commercial $CaCO_3$ (Cano, et al., 2013).

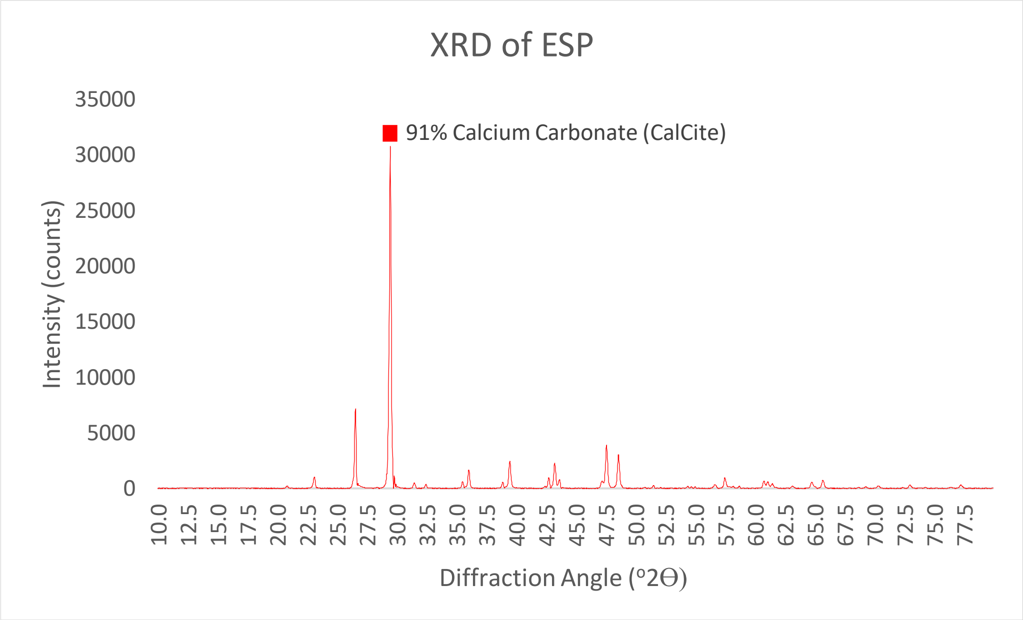

Figure 4.5: XRD pattern of ESP

4.2 Characterization of Composite Film

Table 4.2 and Figure 4.6 shows the FTIR analysis of pure NBR and NBR/ESP composite film. In both NBR and NBR/ESP composite film, the prominent absorption frequency region peaks such as 3200-3500 cm^{-1}, 2840-3000 cm^{-1}, 1580-1650 cm^{-1}, 1350-1480 cm^{-1}, 790-840 cm^{-1}, 665-730 cm^{-1} and 500-600 cm^{-1} remain the same. Carbonate group, CO_3^{-2} which is present in ESP can be found at peaks ranging from 790-840 cm^{-1}. The peaks at 3200-3500 cm^{-1} represent the O-H symmetric stretching vibration, present in the structure of NBR rubber (Sadeghalvaad et al., 2018). Peaks detected in the range of 1580-1650 cm^{-1} shows the presence of nitrile compound in the composite film (Roy et al, 2014). The presence of sulfone stretching bond at peaks 1300-1350 cm^{-1} caused by the interaction of sulphur in the composite film to produce crosslinking (Poonsawat, Poompradub and Ngamcharussrivichai, 2014). The presence of a new band at peaks ranging from 1120-1250cm^{-1} shows that there might be an interaction between NBR rubber and ESP (Ain and Azura, 2010). The band assigned to this peak is C-O-C stretching of ether group.

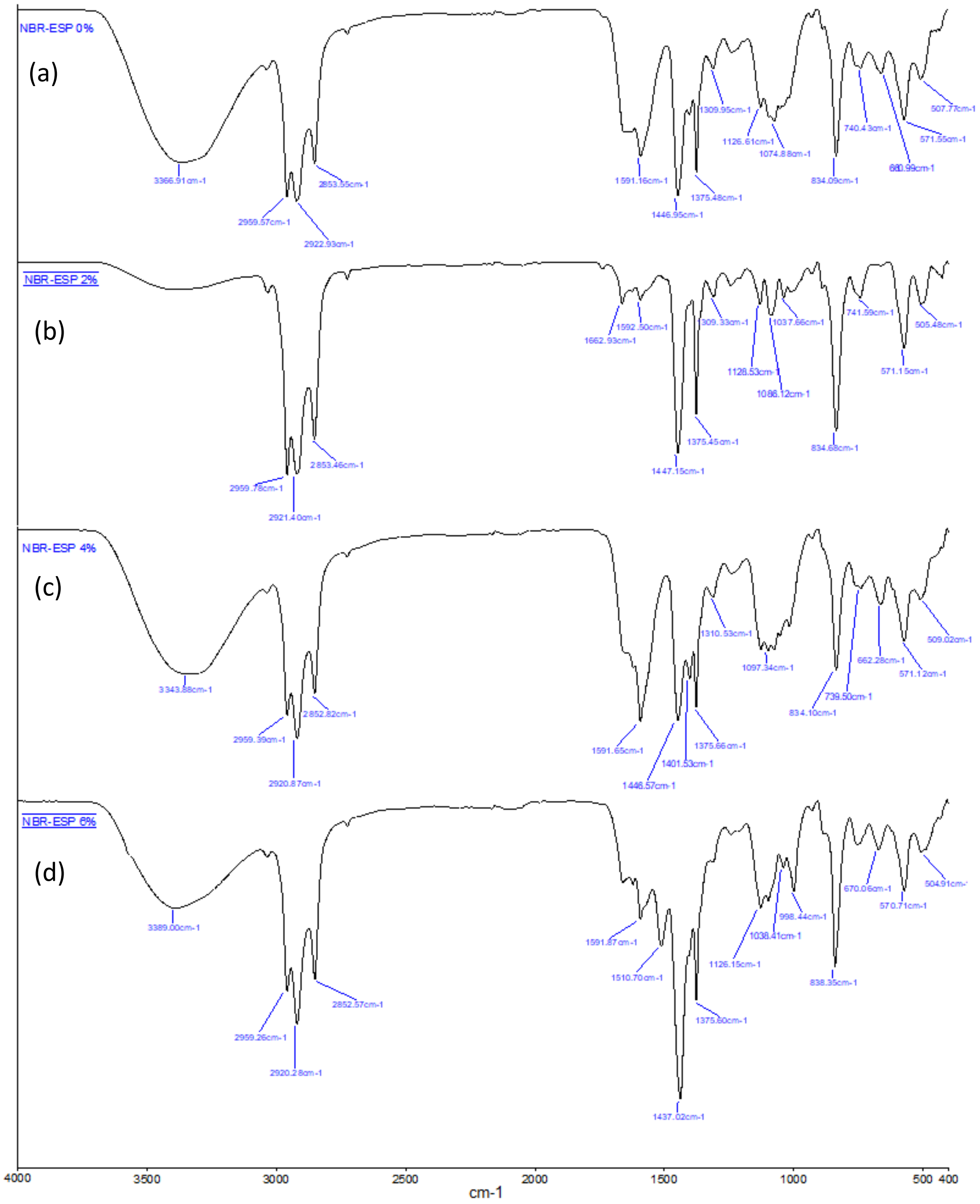

Figure 4.6: FTIR-ATR analysis of (a) 0 phr, (b) 2 phr, (c) 4 phr, (d) 6 phr.

Table 4.2: Absorption Frequency Regions and Functional Group of (a) 0 phr (b) 2 phr (c) 4 phr (d) 6 phr

Absorption Frequency Range (cm^{-1})	Absorption Frequency (cm^{-1})				Functional Group
	NBR	NBR/ESP 2%	NBR/ESP 4%	NBR/ESP 6%	
3200-3550	3366.91		3343.88	3389.00	Alcohol O-H bond stretching
2840-3000	2959.57, 2922.93, 2853.55	2959.78, 2921.40, 2853.46	2959.39, 2920.87, 2852.82	2959.26, 2920.28, 2852.57	Alkane C-H bond stretching
1580-1650	1591.16	1592.50	1591.65	1591.87	Amine N-H bond bending
1350-1480	1446.95	1447.15	1401.53, 1446.57	1437.02	Methyl Group C-H bond bending
1330-1420	1375.48	1375.45	1375.66	1375.60	Alcohol O-H bond bending
1300-1350	1309.95	1309.33	1310.53		Sulfone S=O bond stretching

Figure 4.7 (a), (b), (c) and (d) shows the XRD analysis for pure NBR and NBR/ESP composite film. At pure NBR, intensity peaks can be observed due to the presence of compounding agents such as Sulfur, ZnO, ZMBT and ZDEC. The same intensity peaks can be observed for the NBR/ESP composites. However, as the filler loading increases, a new peak occurs at diffraction angle 30˚. This proves the presence of ESP in the composite film. Higher filler loading shows a higher intensity peak at the same angle position, as the crystalline structure of ESP stays the same throughout the composite film.

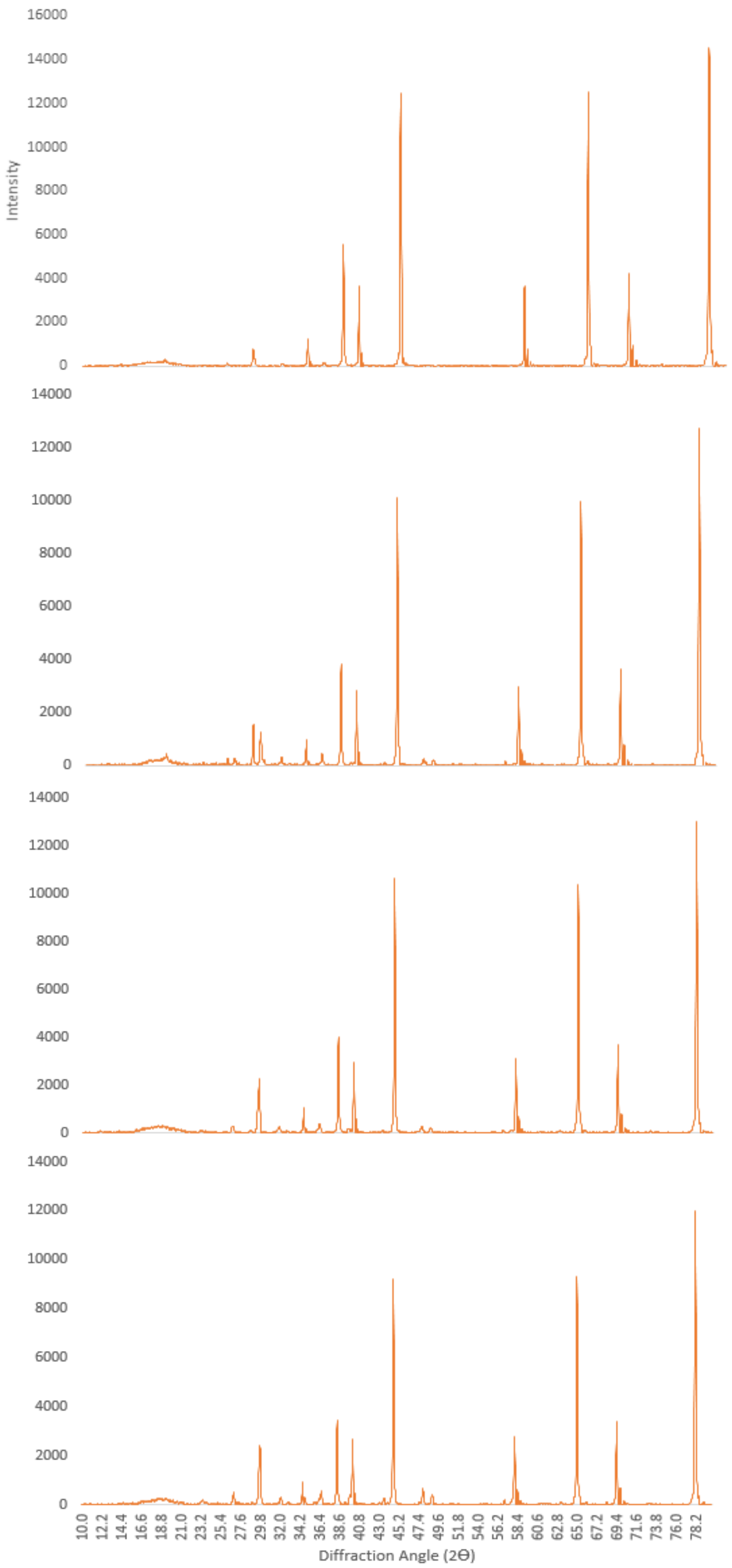

Figure 4.7: XRD of (a) NBR/ESP 0 phr (b) NBR/ESP 2 phr (c) NBR/ESP 4 phr (d) NBR/ESP 6 phr

4.3 Performance Test

4.3.1 Tensile Test and Fracture Surface Analysis

Figure 4.8 shows the ultimate tensile strength (UTS) fo the composite film with different loadings of ESP. The trend line showed continuous increase in tensile strength as the filler loadings increase up to 4 phr. A large increment of 138% was recorded for NBR/ESP 4 phr filler loading compared to pure NBR. However at filler loading 6 phr, the tensile strength of NBR/ESP decreased compared to 4 phr composite, but remain higher than pure NBR. This result suggests that the best dispersion of ESP in NBR was achieved in 4 phr filler loading. The dispersion of ESP filler in NBR matrix is expected to be less at 6 phr loading, compared to 4 phr loading. Improvement of UTS with addition of ESP proves effective stress transfer between NBR matrix and ESP, due to good interaction between the two components. Chemical interaction formation between NBR and ESP has been proven through FTIR analysis in Section 4.1 and 4.2. The irregular shape of ESP fillers as indicated in Figure 4.3 also could promote physical interaction of NBR and ESP. Study has shown that high loadings of $CaCO_3$ filler in NBR with good dispersion showed an increase in tensile strength, while high loadings of $CaCO_3$ filler in NBR with poor dispersion showed a decrease in tensile strength (Sobhy et al., 2003).

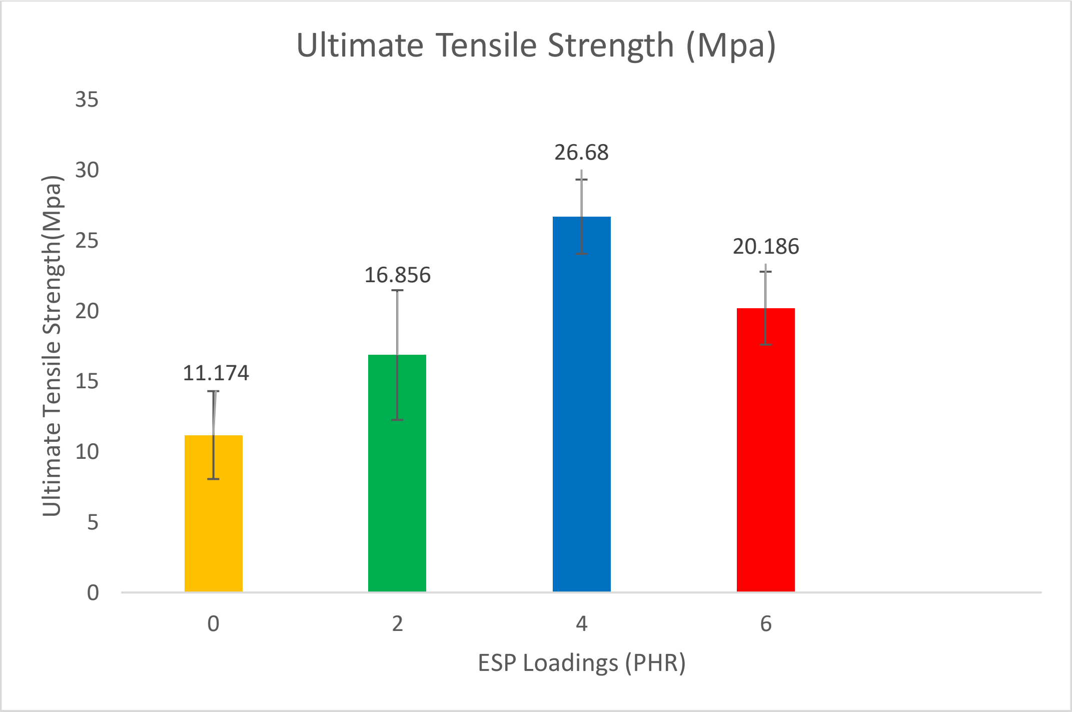

Figure 4.8: UTS of NBR and NBR/ESP composite film

Young's Modulus is used to determine the ability of the composite film to withstand a change in length. Figure 4.9 shows the change in modulus as the filler loadings increased. NBR/ESP of 6 phr had the highest Young's Modulus with value of 0.768 MPa, while pure NBR had the lowest value of 0.456 MPa. Good dispersion of fillers promote more effective surface area for adsorption of polymer chains on the filler's surface. The mechanical interlocking caused demobilization of the polymeric chain, reduce the flexibility and increase the modulus (Sobhy et al., 2003). This result is also supported by the FESEM images of the ESP fillers which indicates irregular surface of filler. This irregular surface of filler will promote physical adsorption and mechanical interlocking of the polymeric chains.

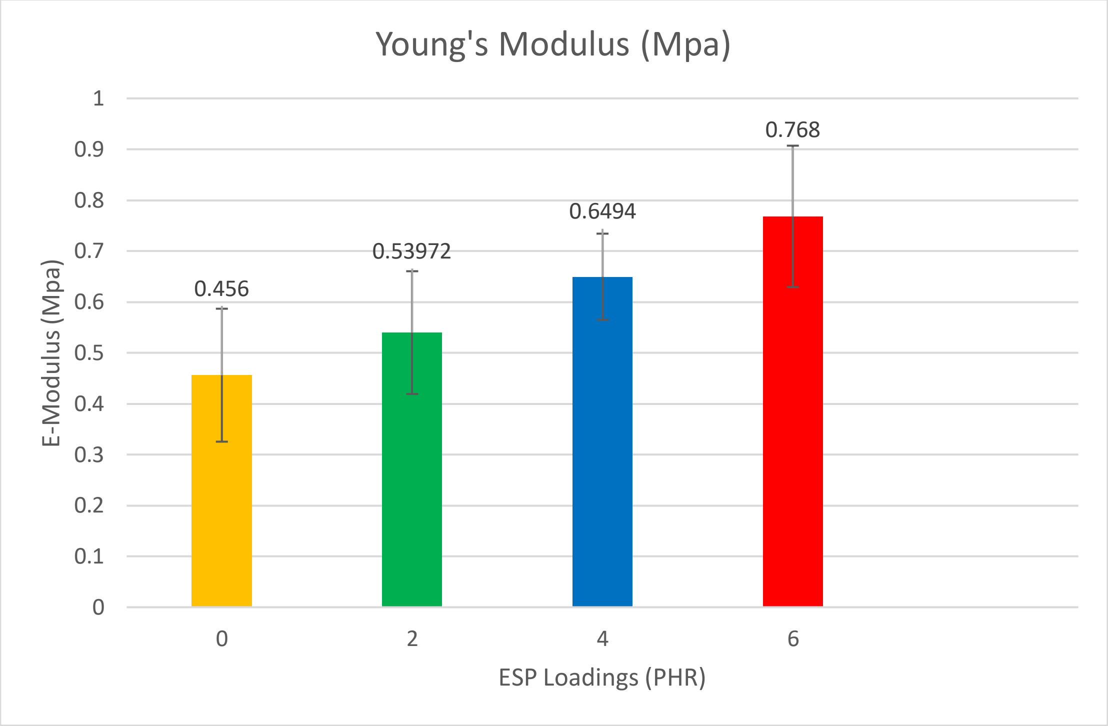

Figure 4.9: Young’s Modulus of NBR and NBR/ESP composite film

Figure 4.10 shows the elongation at break for NBR and NBR/ESP at different filler loadings. The increase in filler loadings shows an increase in elongation at break up to 4 phr filler loadings. However, at NBR/ESP 6 phr, there was a slight decrease in elongation at break, compared to NBR/ESP 4 phr. Pure NBR has the lowest elongation at break value of 852.8 %, while NBR/ESP 4 phr exhibit the highest with the value of 1013.8%. At low filler loading, when dispersion of filler in polymer matrix is good, the filler will be able to move together along the stretched matrix and increase elongation at break (Kapgate and Das, 2014). However as the filler loading increases to 6 phr a reduction of modulus was observed. A portion of rubber matrix is isolated in the agglomerates and was not able to react to stress and strain applied (Ain, Z.N and Azura, A.R., 2010).

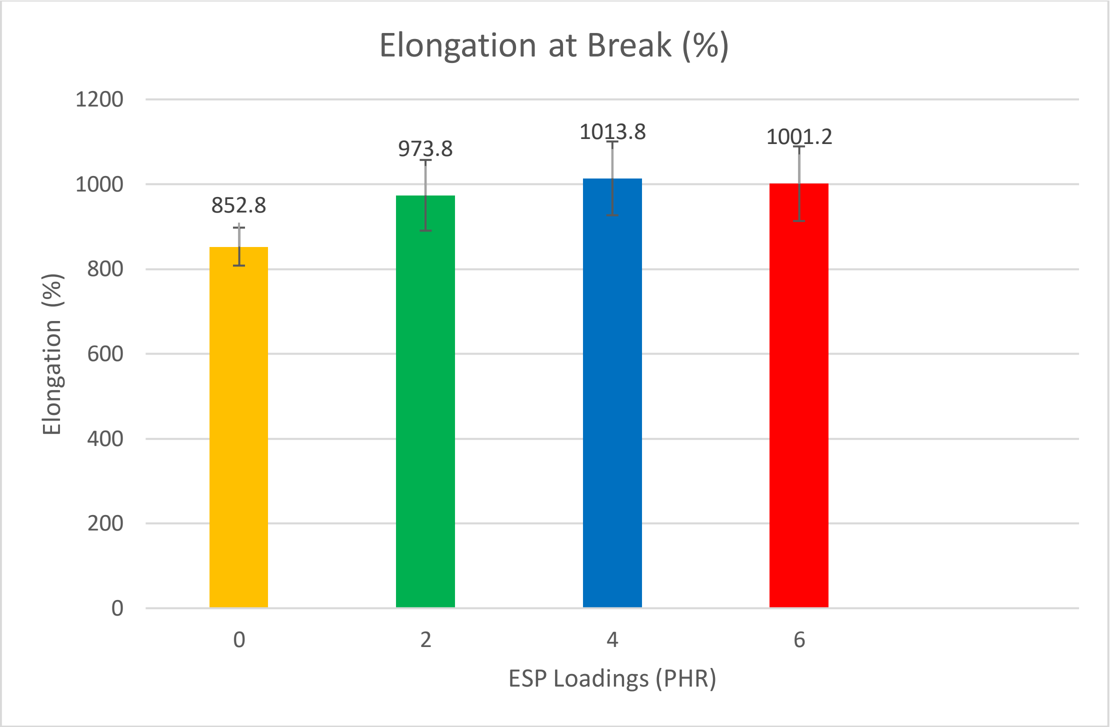

Figure 4.10: Elongation at Break of NBR and NBR/ESP composite film

The FESEM image of NBR/ESP at magnification 2,000× are shown in Figure 4.11. For NBR/ESP, no agglomerates can be observed in the fracture surface of the composite film even up to 6 phr loading. The matrix stretching can be observed in all NBR/ESP samples and circled in red. The presence of matrix stretching leads to high tensile strength and elongation at break. A smaller matrix stretching was observed in NBR/ESP 6 phr which relates to the lower elongation at break for the composite.

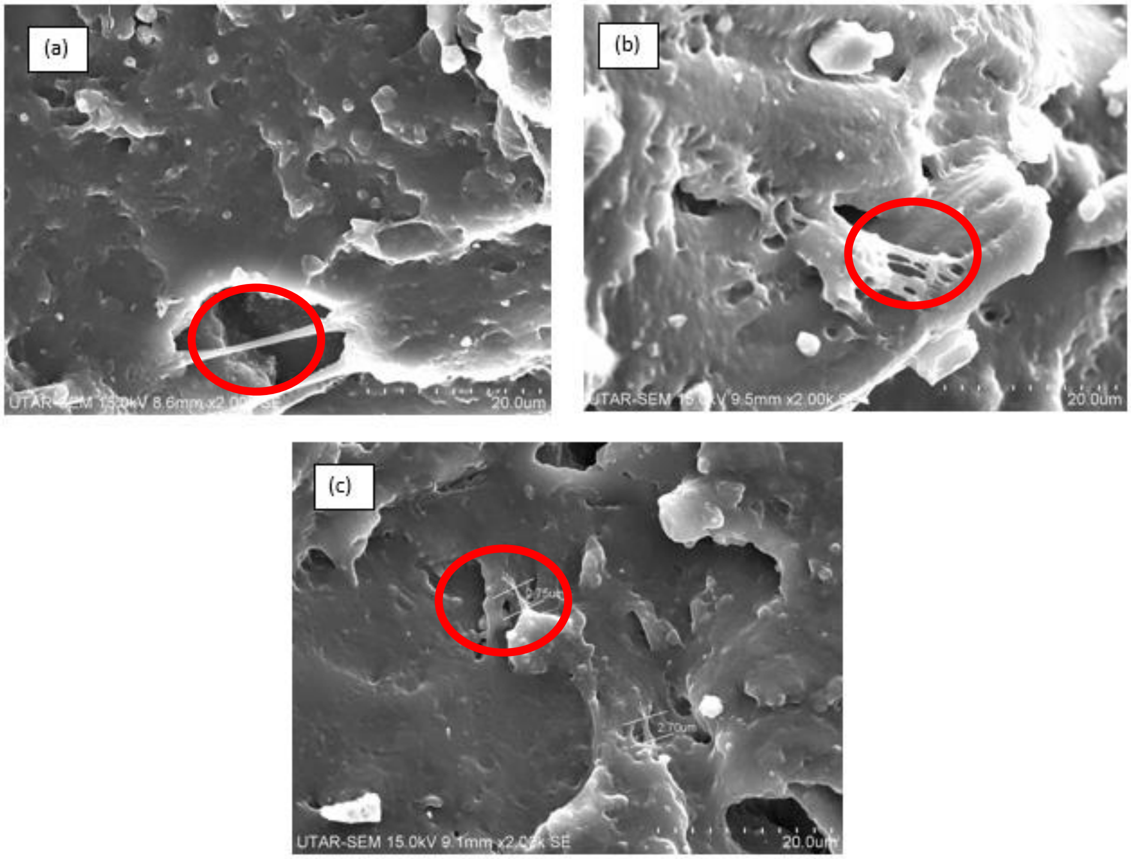

Figure 4.11: FESEM images of (a) NBR/ESP 2 phr (b) NBR/ESP 4 phr (c) NBR/ESP 6 phr

4.3.2 Swelling Test

Figure 4.12 and 4.13 shows the swelling curve of NBR and NBR/ESP at various loadings of ESP in acetone and toluene respectively. Both graph line in Figure 4.12 shows a decrease in the swelling rate as the filler loading increases, with pure NBR having the highest swelling rate of 6.83% and 10.3% at 24 and 72 hours respectively. NBR/ESP 6 PHR shows the lowest swelling rate in acetone with 1.27% and 4.14% at 24 and 72 hours respectively. As for swelling rate in toluene, the rate of swell was much higher for pure NBR, and decreased as the filler loading increases as shown in Figure 4.13. Pure NBR exhibit the highest swelling rate of 360.42% and 400.13% at 24 and 72 hours respectively, while NBR/ESP 6 phr shows the lowest swelling rate in acetone with 330.25% and 336.87% at 24 and 72 hours respectively. Swelling rate is correlated to the crosslink density in a composite film. The results from Figure 4.12 and 4.13 indicates that ESP fillers could promote more crosslinking. Similar effects of fillers in rubber crosslinking was reported by Mostafa et al. (2009), where the increment of filler content in NBR resulted in higher network elasticity in the composite. The higher amount of crosslinks in the composite prevents the extensibility of the rubber chains during swelling, making it harder for solvents to pass through (Mostafa et al., 2009). Increment of crosslinking makes it harder for solvent to diffuse and pass by the gaps of elastomer chain. Figure 4.14 and 4.15 shows the percentage molecular uptake of solvent across the composite film. Both graphs shows a decrease in the uptake as there were more free volume present in the pure NBR due to low crosslinking. Lovely et al (2005), also reported that filler could hinder the solvent uptake by the composite and this effect increases as filler loading increases (Lovely et al., 2005).

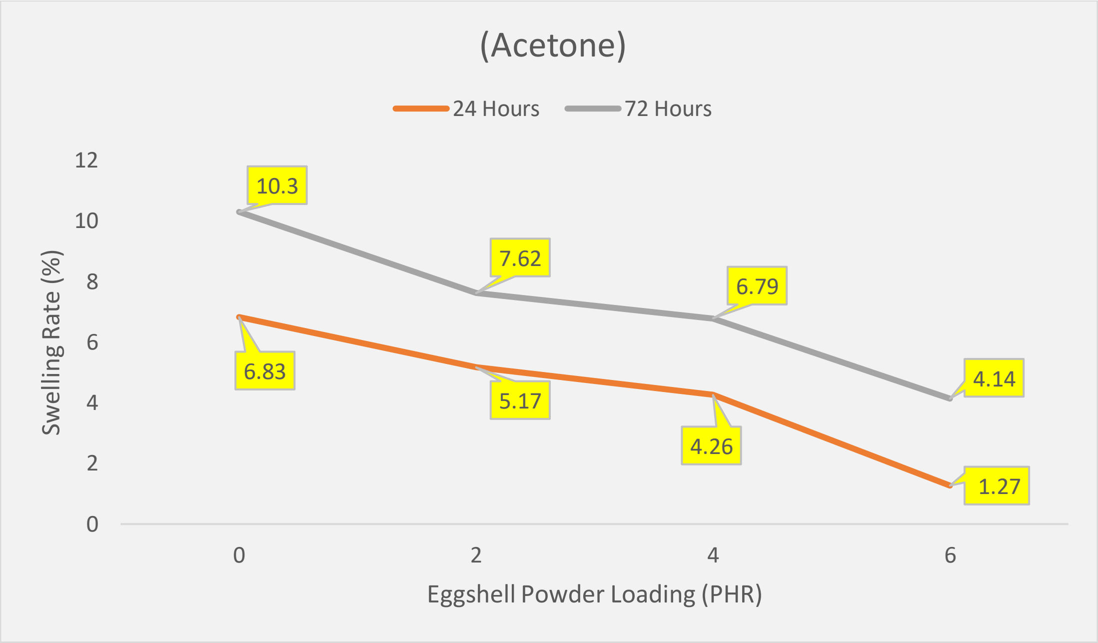

Figure 4.12: Swelling Rate of NBR and NBR/ESP in Acetone

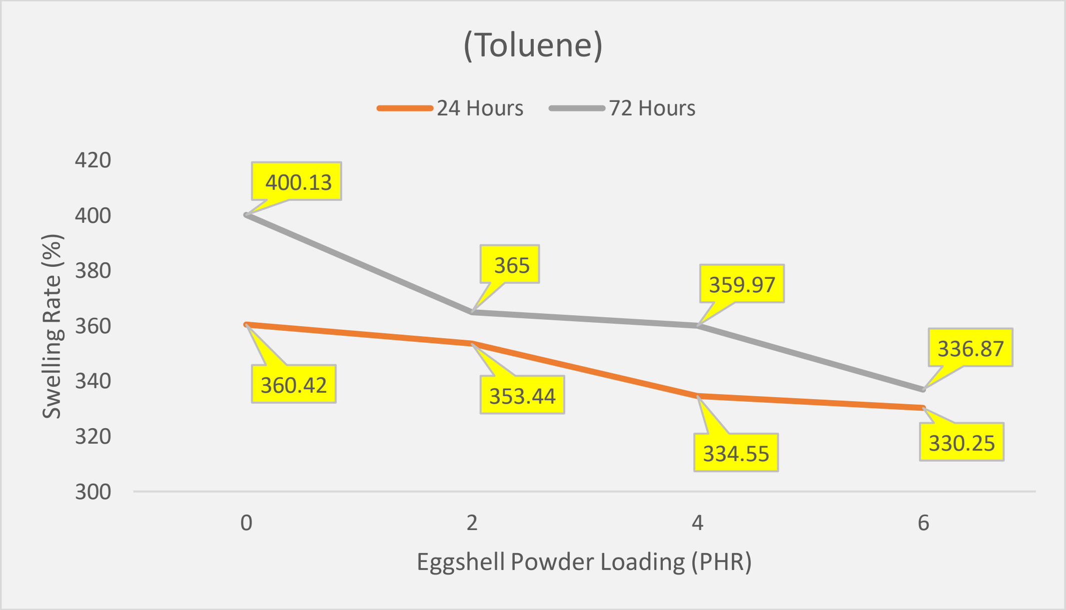

Figure 4.13: Swelling Rate of NBR and NBR/ESP in Toluene

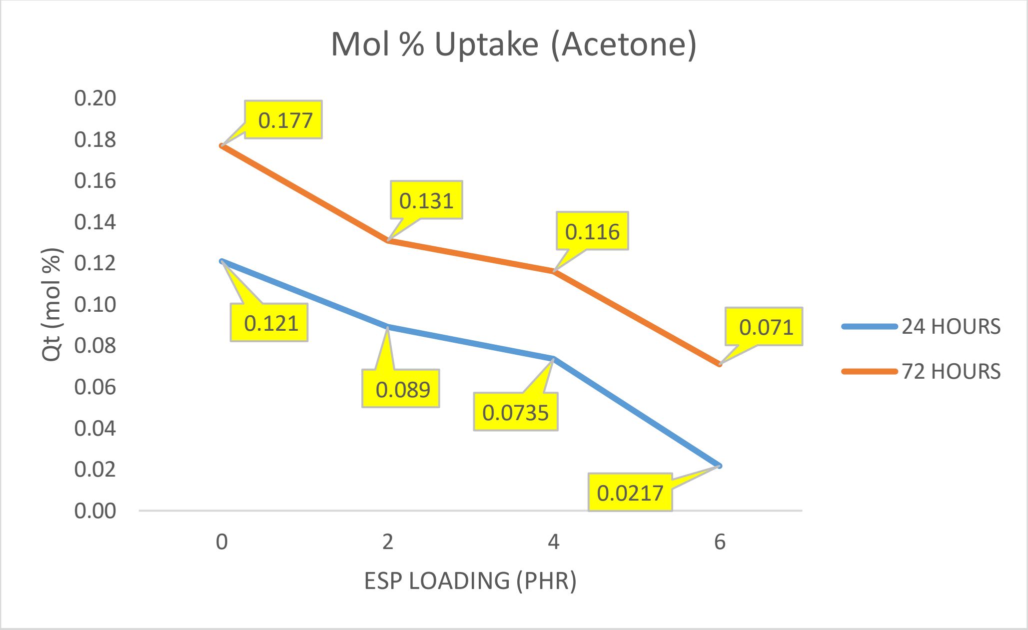

Figure 4.14: Molecular Percent Uptake of NBR and NBR/ESP in Acetone.

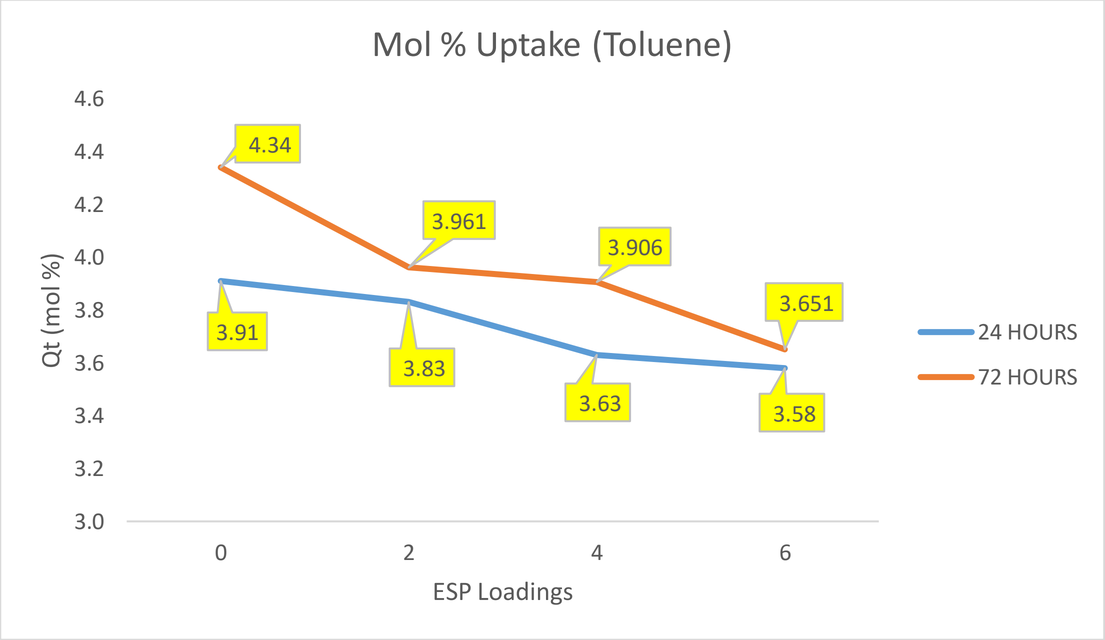

Figure 4.15: Molecular Percent Uptake of NBR and NBR/ESP in Toluene.

4.3.3 Chemical Degradation

Figure 4.16 and 4.17 shows the chemical degradation of NBR and NBR/ESP with different loadings of fillers in various chemicals. The rate of degradation decreases as the filler loading increases. Pure NBR has the highest rate of chemical degradation, while NBR/ESP 6 phr has the lowest rate of chemical degradation. When studying the chemical degradation, factors that need to be considered are the solvent uptake across film and barrier properties of the filler. The penetration of solvent depends widely on the availability of free space in NBR matrix to accommodate the penetration of molecule. Higher filler loading reduces the free volume present in the composite film, lowering the ability of rubber matrix to accommodate the solvent penetration (Balachandran and Bhagawan, 2012). The presence of filler also acts as a barrier and in this case the presence of $CaCO_3$ in ESP which is an isotropic filler makes it hard to permeate (Ge and Aldi, 2015). Higher filler loading in NBR/ESP reduces the mobilization of polymer chain, making it harder for solvents to penetrate through the composite film.

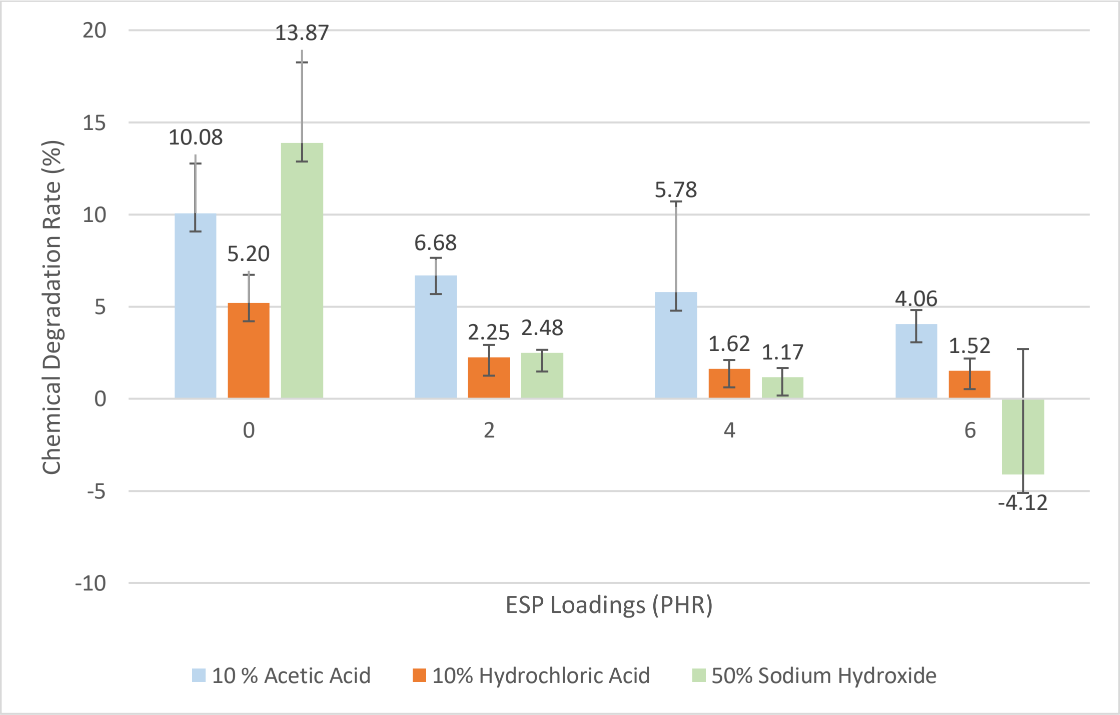

Figure 4.16: Chemical Degradation of NBR and NBR/ESP upon exposure to different chemicals

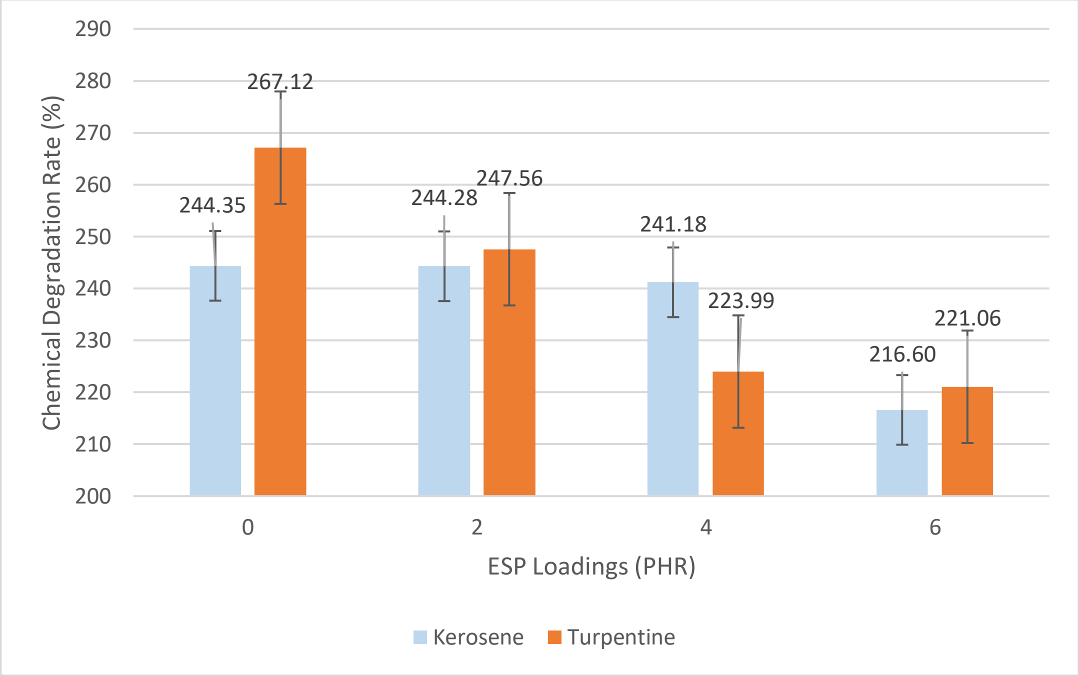

Figure 4.17: Chemical Degradation of NBR and NBR/ESP upon exposure to different chemicals

4.3.4 Crosslinking Density

Figure 4.18 shows the crosslinking density of NBR and NBR/ESP at different filler loadings. Higher filler loading increases the crosslink in composite film. NBR/ESP at 6 phr has the highest crosslink density, while pure NBR has the lowest crosslinking density. ESP plays a physical crosslink role in the polymer which increases hardness and also Young's Modulus of composite film. The well dispersion of ESP in NBR brings the elastomer chains closer and packed, reducing free volume and keeping the chains intact with the filler. The crosslinking density is correlated to the swelling of composite film. A higher crosslink in composite film hinders the movement of solvent in the elastomer chain, reducing its swelling. This results are in accordance the results in Section 4.3.1-4.3.4.

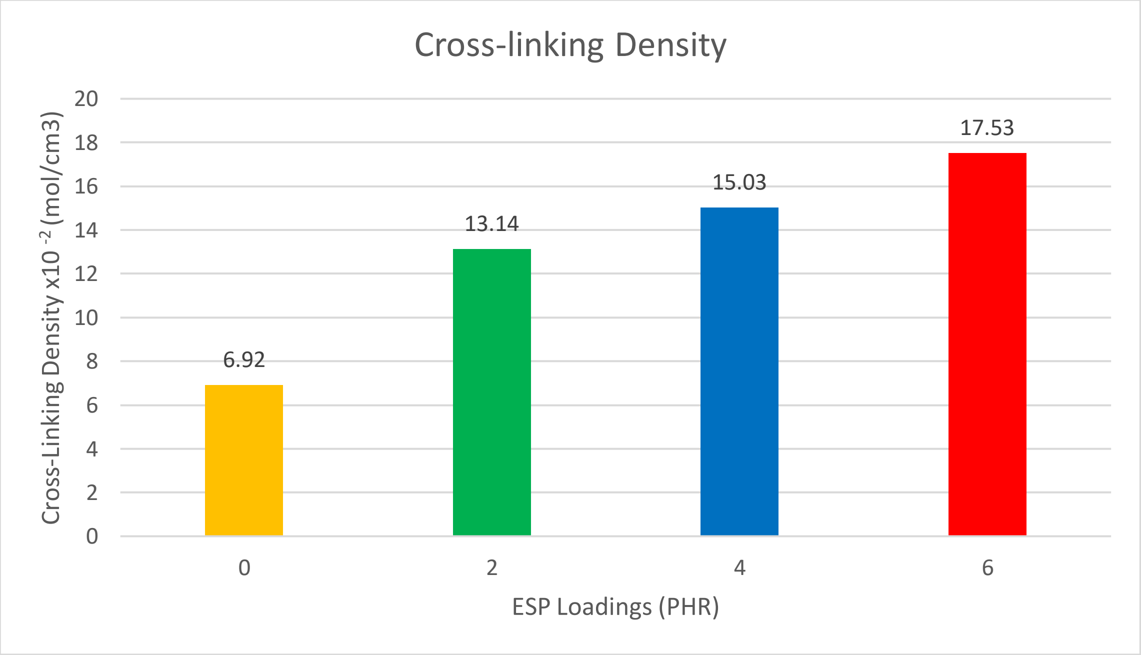

Figure 4.18: Crosslinking Density of NBR and NBR/ESP at Different Loadings

CHAPTER 5

CONCLUSION AND RECOMMENDATION

5.1 Conclusion

ESP has been prepared and the characterization of ESP has been conducted. Characterization analysis for ESP such as PSA, TGA, FTIR, FESEM and XRD proves that ESP can be a suitable replacement for the commercial $CaCO_3$.

NBR and NBR/ESP composite film were prepared using the latex compounding method and the characterization test was done for the composite film. Performance test which included tensile test, swelling test, crosslinking density test and chemical degradation were conducted to determine the effect of ESP loadings on the performance of composite film.

The optimum UTS, elongation a break and modulus value has been achieved at 4 phr loading. Crosslinking density of composite film increased as filler loading increased, due to the closely packed elastomer chains. Swelling rate and chemical degradation of composite film reduced as filler loading increased, due to the high crosslink and barrier effect of filler in composite filler.

The factors that influence the performance of composite film is the good dispersion of ESP filler in NBR matrix and also the increment of crosslink in composite film. Thus from this research, NBR/ESP composite film with 4-6 phr ESP loadings has a large potential to be used as a glove material.

5.2 Recommendations

Several recommendations can be made to be implemented in future researches

- Comparison in performance of composite film using ESP and nano-ESP filler.
- Studies done on the optimum temperature and optimum curing time to improve the performance of composite film
- Study the effect of filler size on thermal properties of composite film.

REFERENCES

Ahmad, R., Rohim, R. and Ibrahim, N. (2015). Properties of Waste Eggshell as Calcium Oxide Catalyst. *Applied Mechanics and Materials*, 754-755, pp.171-175.

Ain, Z. and Azura, A. (2010). Effect of different types of filler and filler loadings on the properties of carboxylated acrylonitrile-butadiene rubber latex films. *Journal of Applied Polymer Science*, 119(5), pp.2815-2823.

Arvanitoyannis, I. (2008). *Waste management for the food industries*. Amsterdam: Academic Press.

Balachandran, M. and Bhagawan, S. (2012). Mechanical, thermal, and transport properties of nitrile rubber-nanocalcium carbonate composites. *Journal of Applied Polymer Science*, 126(6), pp.1983-1992.

Baláž, M. (2014). Eggshell membrane biomaterial as a platform for applications in materials science. *Acta Biomaterialia*, 10(9), pp.3827-3843.

Bawadukji NA, Jabra R. Formulation, Preparation, and Mechanical Characterization of Nitrile-Butadiene Rubber (NBR) Composites. Mater Sci Ind J. 2017;15(1):116.

Bootklad, M. and Kaewtatip, K. (2013). Biodegradation of thermoplastic starch/eggshell powder composites. *Carbohydrate Polymers*, 97(2), pp.315-320.

Boronat, T., Fombuena, V., Garcia-Sanoguera, D., Sanchez-Nacher, L. and Balart, R. (2015). Development of a biocomposite based on green polyethylene biopolymer and eggshell. Materials & Design, 68, pp.177-185.

Brewis, D., Briggs, D. and Pritchard, G. (2012). *Plastics Additives*. 2nd ed. Dordrecht: Springer Netherlands.

Budhiarta, I., Siwar, C. and Basri, H. (2012). Current Status of Municipal Solid Waste Generation in Malaysia. International Journal on Advanced Science, Engineering and Information Technology, 2(2), p.129.

Brun, L., Lupo, M., Delorenzi, D., Di Loreto, V. and Rigalli, A. (2013). Chicken eggshell as suitable calcium source at home. International Journal of Food Sciences and Nutrition, 64(6), pp.740-743.

Carr, F. and Frederick, D. (2000). Calcium Carbonate. *Kirk-Othmer Encyclopedia of Chemical Technology*.

Chakraborty, S., Bandyopadhyay, S., Ameta, R., Mukhopadhyay, R. and Deuri, A. (2007). Application of FTIR in characterization of acrylonitrile-butadiene rubber (nitrile rubber). *Polymer Testing*, 26(1), pp.38-41.

Charles Grimm, D. (1998). *Method for the Production of Nitrile Rubber*. 5708132.

Cheremisinoff, N. (1993). *Elastomer technology handbook*. 1st ed. Boca Raton, Fla.: CRC Press.

Cheremisinoff, N. (1997). Handbook of engineering polymeric materials. 1st ed. New York: M. Dekker.

Ciesielski, A. (2001). An introduction to rubber technology. 1st ed. Shawbury, Shrewsbury, Shropshire, U.K: Rapra Technology Ltd.

Cordeiro, C. M.; Hincke, M. T. Recent Patents on Eggshell: Shell and Membrane Applications. Recent Pat. Food, Nutr. Agric. 2011, 3(1), 1-8

De, S., White, J. and Naskar, K. (2009). *Rubber technologist's handbook*. 2nd ed. Shrewsbury: Rapra Technology Ltd.

Dennis, J., Xiao, S., Agarwal, M., Fink, D., Heuer, A. and Caplan, A. (1996). Microstructure of matrix and mineral components of eggshells from White Leghorn chickens (Gallus gallus). *Journal of Morphology*, 228(3), pp.287-306.

Erman, B., Mark, J. and Roland, C. (2013). *The science and technology of rubber*. 4th ed. Waltham, Mass.: Academic Press.

Flores-Cano, J., Leyva-Ramos, R., Mendoza-Barron, J., Guerrero-Coronado, R., Aragón-Piña, A. and Labrada-Delgado, G. (2013). Sorption mechanism of Cd(II) from water solution onto chicken eggshell. *Applied Surface Science*, 276, pp.682-690.

Fombuena, V., Bernardi, L., Fenollar, O., Boronat, T. and Balart, R. (2014). Characterization of green composites from biobased epoxy matrices and bio-fillers derived from seashell wastes. *Materials & Design*, 57, pp.168-174

Fu, S., Feng, X., Lauke, B. and Mai, Y. (2008). Effects of particle size, particle/matrix interface adhesion and particle loading on mechanical properties of particulate–polymer composites. *Composites Part B: Engineering*, 39(6), pp.933-961.

Freire, M. and Holanda, J. (2006). Characterization of avian eggshell waste aiming its use in a ceramic wall tile paste. *Cerâmica*, 52(324), pp.240-244.

Gerard, J. (2001). *Fillers and filled polymers*. 2nd ed. Weinheim: Wiley-VCH.

Ge, C. and Aldi, R. (2013). Effects of aragonite calcium carbonate on barrier and mechanical properties of a three-layer co-extruded blown low-density polyethylene film. *Journal of Plastic Film & Sheeting*, 30(1), pp.77-90.

Ghabeer, T., Dweiri, R. and Al-Khateeb, S. (2012). Thermal and mechanical characterization of polypropylene/eggshell biocomposites. *Journal of Reinforced Plastics and Composites*, 32(6), pp.402-409.

Ghosh, P., Fawcett, D., Sharma, S. and Poinern, G. (2016). Progress towards Sustainable Utilisation and Management of Food Wastes in the Global Economy. https://www.hindawi.com/journals/ijfs/2016/3563478/.

Hassan, S. and Aigbodion, V. (2015). Effects of eggshell on the microstructures and properties of Al–Cu–Mg/eggshell particulate composites. *Journal of King Saud University - Engineering Sciences*, [online] 27(1), pp.49-56. Available at: https://www.sciencedirect.com/science/article/pii/S1018363913000093 [Accessed 16 Mar. 2019].

Hassen, A., Dizbay-Onat, M., Bansal, D., Bayush, T. and Vaidya, U. (2015). Utilization of Chicken Eggshell Waste as a Bio-Filler for Thermoplastic Polymers: Thermal and Mechanical Characterization of Polypropylene Filled with Naturally Derived CaCo3. *Polymers and Polymer Composites*, [online] 23(9), pp.653-662. Available at: https://www.researchgate.net/publication/284187876_Utilization_of_Chicken_Eggshell_Waste_as_a_Bio-Filler_for_Thermoplastic_Polymers_Thermal_and_Mechanical_Characterization_of_Polypropylene_Filled_With_Naturally_Derived_CaCO3

Iyer, K. and Torkelson, J. (2014). Green composites of polypropylene and eggshell: Effective biofiller size reduction and dispersion by single-step processing with solid-state shear pulverization. *Composites Science and Technology*, 102, pp.152-160.

Katz, H. and Milewski, J. (1987). Handbook of fillers for plastics. 1st ed. New York: Van Nostrand Reinhold Co.

Kang, J., Kotaki, M., Okubayashi, S. and Sukigara, S. (2010). Fabrication of electrospun eggshell membrane nanofibers by treatment with catechin. *Journal of Applied Polymer Science*, 117(4), pp.2042-2049.

Kapgate, B. and Das, C. (2014). Filler–filler and rubber–filler interactions in nitrile rubber/silica composites. *Emerging Materials Research*, 3(1), pp.46-51.

Keller, R. (2012). *Practical guide to hydrogenated nitrile butadiene rubber technology*. 1st ed. Shropshire, U.K.: Smithers Rapra.

Kitamura, M. (2001). Crystallization and Transformation Mechanism of Calcium Carbonate Polymorphs and the Effect of Magnesium Ion. *Journal of Colloid and Interface Science*, 236(2), pp.318-327.

Li-Chan, E. C. Y.; Powrie, W. D.; Nakai, S. The chemistry of eggs and egg products. In Egg Science and Technology, Stadelman W. J., Cotterill O. J., Ed., Haworth Press: New York, 1995; p 105.

Maloneytech. (2013). [online] Available at: https://www.maloneytech.com/wp-content/uploads/2013/04/Rubber-Properties-Chart.pdf [Accessed 24 Apr. 2019].

Mantia, F., Morreale, M. and Ishak, Z. (2005). Processing and mechanical properties of organic filler-polypropylene composites. *Journal of Applied Polymer Science*, [online] 96(5), pp.1906-1913. Available at: https://onlinelibrary.wiley.com/doi/abs/10.1002/app.21623 [Accessed 16 Mar. 2019].

Mark, J., Erman, B. and Roland, M. (2013). *The science and technology of rubber*. Amsterdam ;: Elsevier Academic Press.

Mascia, L. (1974). *The role of additives in plastics*. 2nd ed. London: Arnold.

Mohanty, A., Misra, M. and Druzal, L. (2005). *Natural fibers, biopolymers, and their biocomposites*. 1st ed. Boca Raton, FL: CRC Press.

Mostafa, A., Abouel-Kasem, A., Bayoumi, M. and El-Sebaie, M. (2009). Effect of carbon black loading on the swelling and compression set behavior of SBR and NBR rubber compounds. *Materials & Design*, 30(5), pp.1561-1568.

Naemchanthara, K., Meejoo, S., Onreabroy, W. and Limsuwan, P. (2008). Temperature Effect on Chicken Egg Shell Investigated by XRD, TGA and FTIR. *Advanced Materials Research*, 55-57, pp.333-336.

Nagdi, K. (1993). *Rubber as an engineering material*. Munich: Hanser Publ.

NBR market worth dollar;1393.0 million by 2022 forecasts study. (2018). *Sealing Technology*, 2018(10), pp.4-5.

N. Gent, A. (2016). *Rubber | chemical compound*. [online] Encyclopedia Britannica. Available at: https://www.britannica.com/science/rubber-chemical-compound [Accessed 16 Mar. 2019].

Poonsawat, W., Poompradub, S. and Ngamcharussrivichai, C. (2014). Preparation of sulfonic acid-containing rubbers from natural rubber vulcanizates. *International Conference on Experimental Mechanics 2013 and Twelfth Asian Conference on Experimental Mechanics*.

Ramdani, N., Wang, J., He, X., Feng, T., Xu, X., Liu, W. and Zheng, X. (2014). Effect of crab shell particles on the thermomechanical and thermal properties of polybenzoxazine matrix. *Materials & Design*, 61, pp.1-7.

Rothon, R. (2002). *Particulate fillers for polymers*. Shawbury, U.K.: Rapra Technology Ltd.

T, M., Ramezani-Dakhel, H. and Sarami, R. (2010). Improving Thermo-mechanical Properties of Styrene Butadiene Rubber Nanocomposites Using Eggshell Bio-filler. *2010 Fourth International Conference on Quantum, Nano and Micro Technologies*.

Shi G Z H; Nedea C (1994) Antec '94. Conference Proceedings. San Francisco, Ca., 1st-5th May 1994, Vol.II, p.2488- 93. 012

Sobhy, Maged & El-Nashar, Doaa & Maziad, Nabila. (2003). Cure Characteristics and Physicomechanical Properties of Calcium Carbonate Reinforcement Rubber Composites. Egypt. J. Sol., Vol. (26), No. (1), (2003). 26.

Somdee, P. and Hasook, A. (2017). Effect of modified eggshell powder on physical properties of poly(lactic acid) and natural rubber composites. *Materials Today: Proceedings*, 4(5), pp.6502-6511.

Statista. (2018). *Global natural and synthetic rubber consumption 1990-2018*. [online] Available at: https://www.statista.com/statistics/275399/world-consumption-of-natural-and-synthetic-caoutchouc/ [Accessed 16 Mar. 2019].

Stevulova, N., Schwarzova, I., Terpakova, E. and Singovszka, E. (2015). Optimization of organic filler properties by its physical treatment. *Journal of Civil Engineering, Environment and Architecture*, XXXII (4/2015), pp.427-433.

Tangboriboon, N., Pannangpetch, W., Aranyik, K., Petcharoen, K. and Sirivat, A. (2015). Embedded Eggshells as a Bio-Filler in Natural Rubber for Thermal Insulation Composite Foams. Progress in Rubber Plastics and Recycling Technology, 31(3), pp.189-205.

Technology of rubber and allied products. (2013). Delhi: National Institute of Industrial Research.

Toro, P., Quijada, R., Yazdani-Pedram, M. and Arias, J. (2007). Eggshell, a new bio-filler for polypropylene composites. *Materials Letters*, 61(22), pp.4347-4350.

Tsai, W., Yang, J., Lai, C., Cheng, Y., Lin, C. and Yeh, C. (2006). Characterization and adsorption properties of eggshells and eggshell membrane. *Bioresource Technology*, 97(3), pp.488-493.

Wypych, G. (2004). *Handbook of plasticizers*. 1st ed. Toronto: ChemTec.

Xanthos, M. (2010). *Functional fillers for plastics*. 1st ed. Weinheim: Wiley-VCH.

APPENDICES

APPENDIX A: FTIR RESULT

(a) Pure NBR

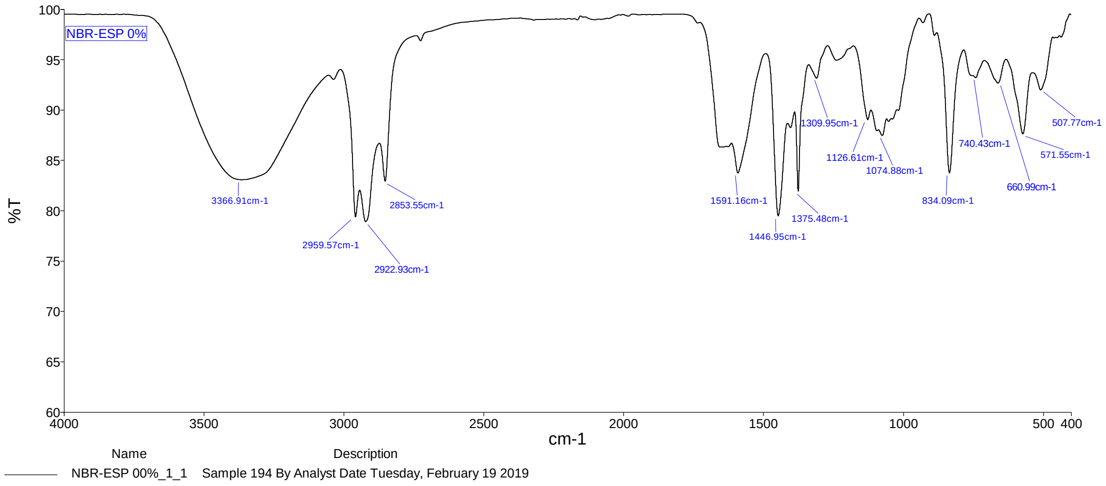

(b) NBR/ESP 2 PHR

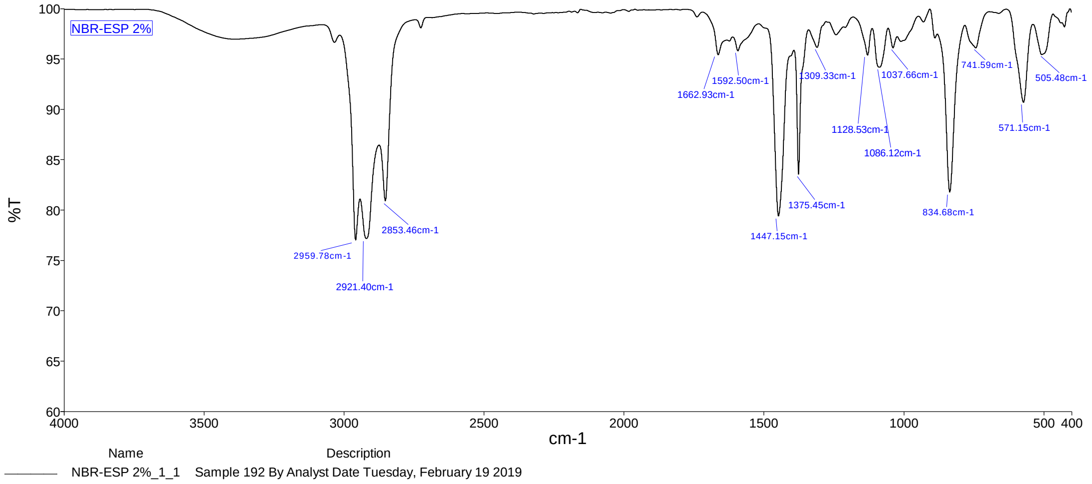

(c) NBR/ESP 4 PHR

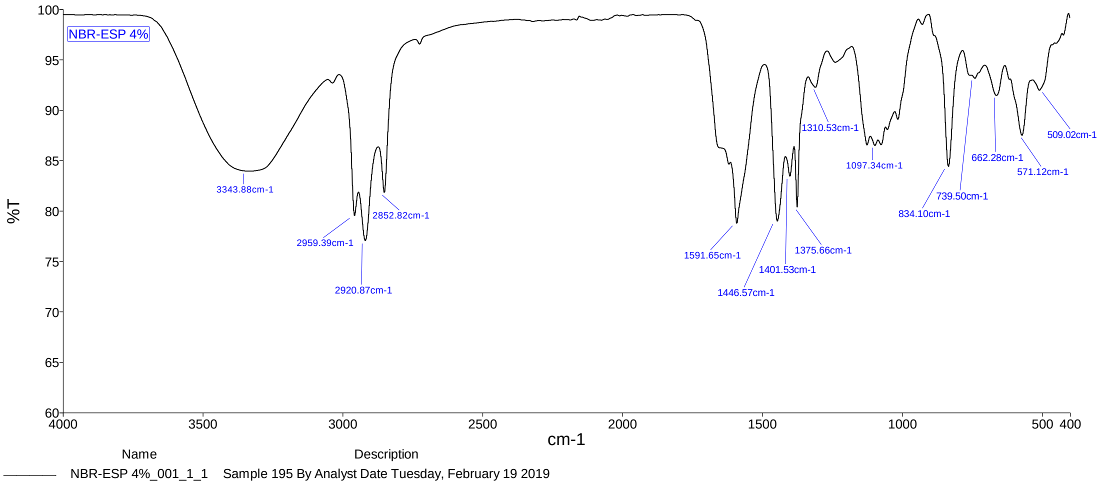

(d) NBR/ESP 6 PHR

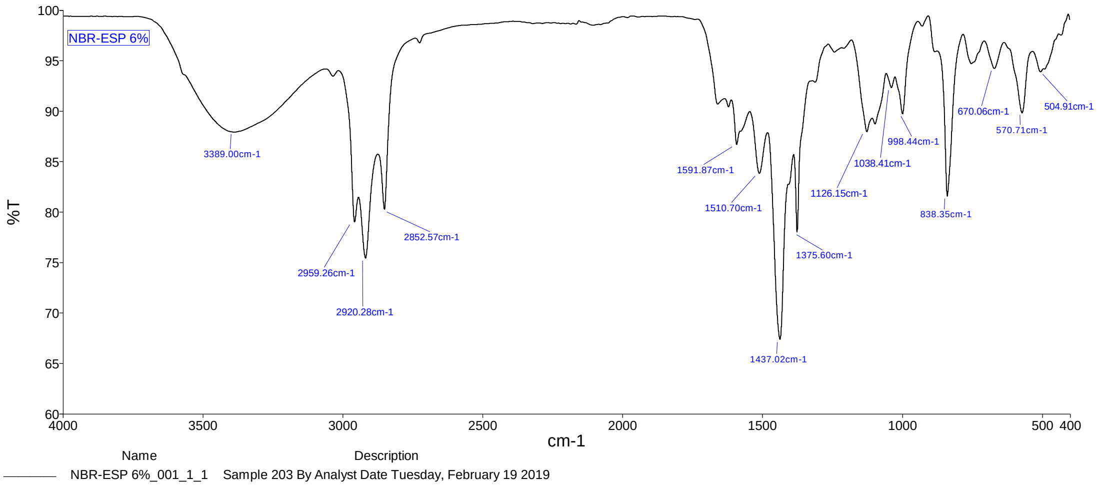

APPENDIX B: FESEM RESULT

(a) ESP

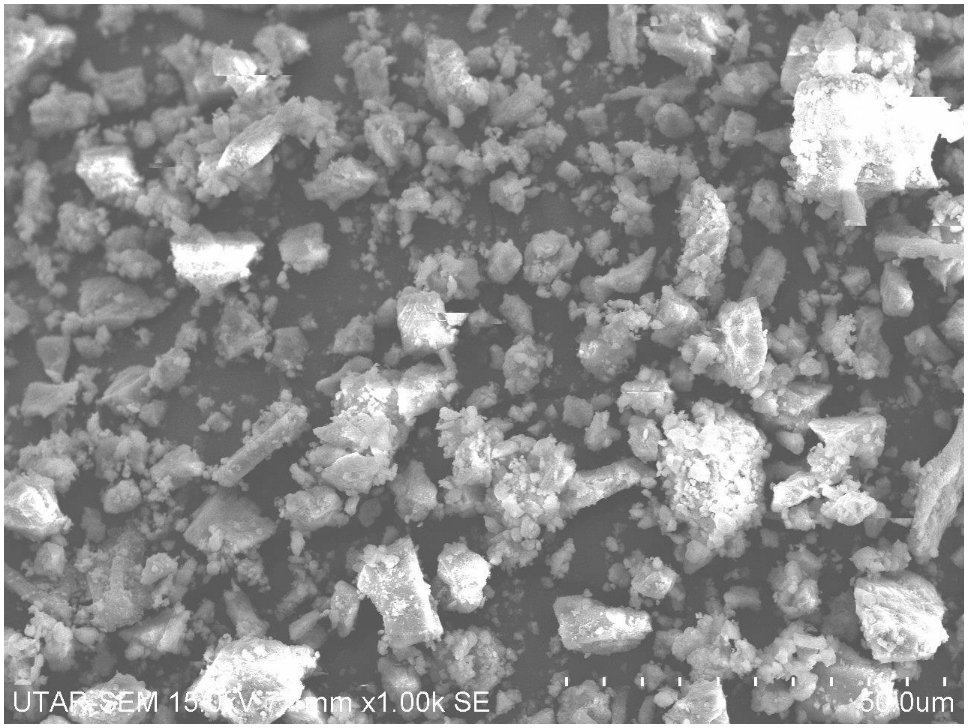

(b) NBR/ESP 2 PHR

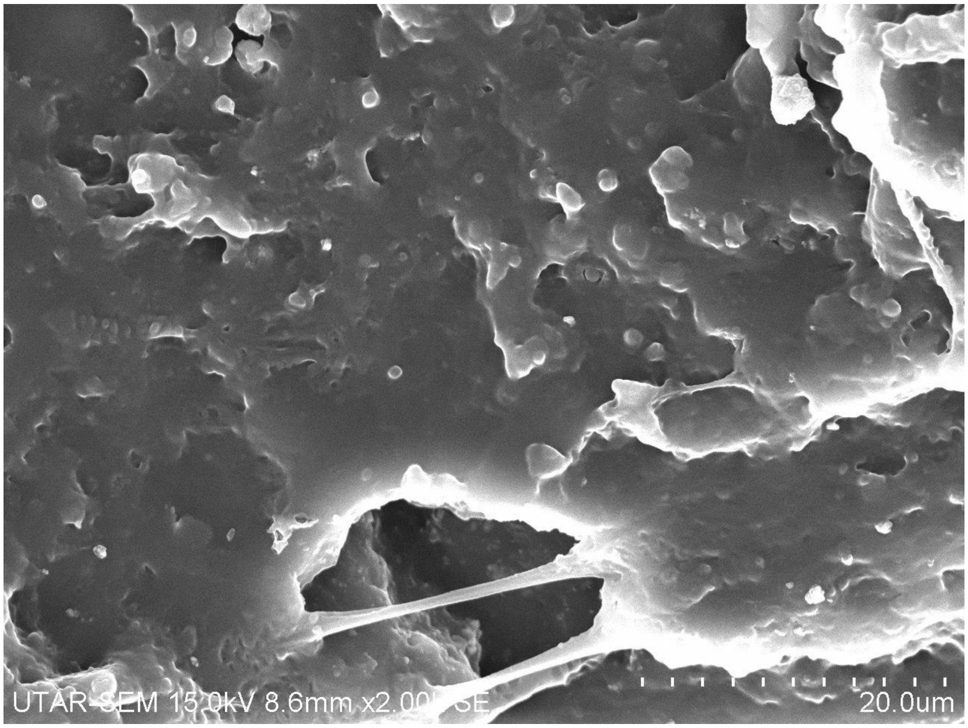

(c) NBR/ESP 4 PHR

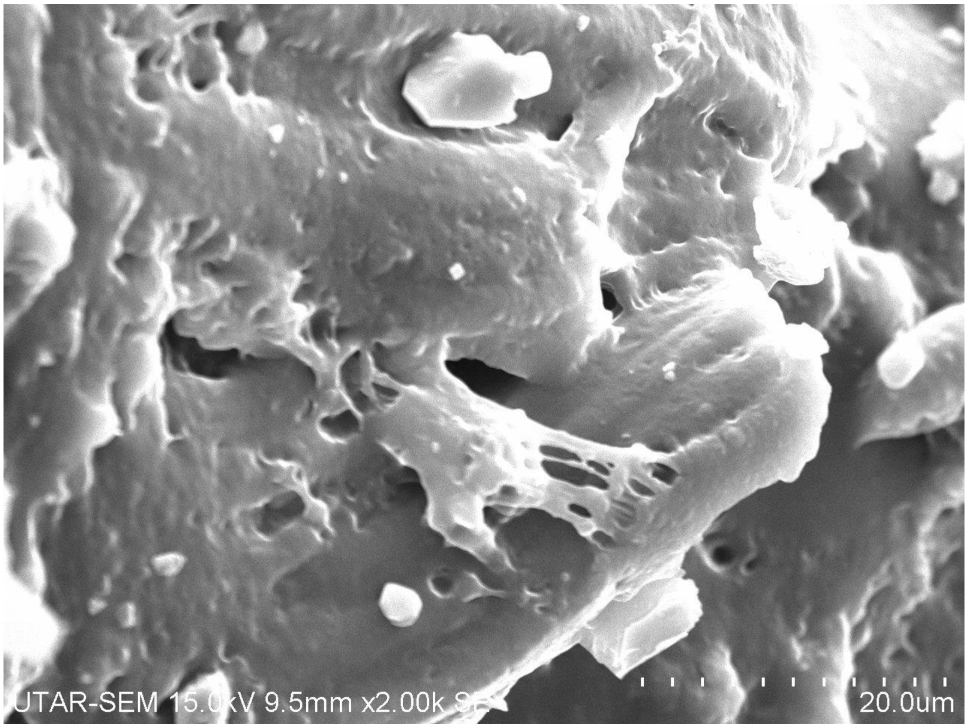

(d) NBR/ESP 6 PHR